Zoosyst. Evol. 101 (4) 2025, 2387–2403 | DOI 10.3897/zse.101.170704

PENSOFT

für Naturkunde MUSEUM FÜR NATURKUNDE BERLIN

A new species of *Alticola* (Mammalia, Rodentia, Arvicolinae) from southern Tibet, China

Ming Kun Tang[1,2,3], Hong Qiu[1,2,3], Bu Qing Peng[1,2,3], Rui Liao[1,2,3], Robert W. Murphy[4], Xu Ming Wang[1,2,3], Xuan Pan[1,2,3], Xin Wang[1,2,3], Shao Ying Liu[1,2,3]

1 *Sichuan Key Laboratory of Ecological Restoration and Conservation for Forest and Wetland, Sichuan Academy of Forestry, Chengdu 610081, China*

2 *Sichuan Giant Panda National Park Observation and Research Station, Sichuan Academy of Forestry, Aba Tibetan and Qiang Autonomous Prefecture 623006, China*

3 *Wolong Forest Ecology Observation and Research Station of Sichuan, Sichuan Academy of Forestry, Aba Tibetan and Qiang Autonomous Prefecture 623006, China*

4 *Department of Natural History, Royal Ontario Museum, Toronto M5S 2C6, Canada*

https://zoobank.org/2AB54569-1546-43B1-9965-76503240F4A6

Corresponding author: Shao Ying Liu (shaoyliu@163.com)

Academic editor: M. T. R. Hawkins ♦ **Received** 1 September 2025 ♦ **Accepted** 19 November 2025 ♦ **Published** 3 December 2025

Abstract

The complex topography and diverse habitats of the Qinghai-Tibet Plateau have made it a center of speciation and evolution for various taxa, including small mammals. Our surveys in 2008 and 2023 on the southern part of the plateau discovered a population of mountain voles (genus *Alticola*) not assignable to any known species. Specimens were collected from shrublands near streams (at elevations of 3,228–4,022 m) in Longzi and Lang counties, Tibet. Integrative taxonomic analyses, incorporating molecular phylogenetics and morphology, confirmed their distinct status. They form a well-supported clade that is sister to *A. stoliczkanus*, from which it diverged approximately 0.49 Mya (95% HPD interval: 0.20–0.77). Kimura-2-parameter distances for the complete cytochrome *b* gene between these individuals and other nominal species of *Alticola* range from 4.0% to 10.3%. Morphologically, this unique lineage is diagnosed by possessing the simplest M^3 with a truncated posterior lobe, a slender tail, darker pelage, and distinctive bacular characteristics. We describe this lineage as *Alticola yarlungia* **sp. nov.** This discovery suggests that species diversity within genus *Alticola* remains underestimated and underscores the need for continued biodiversity exploration in the eastern Himalayan region.

Key Words

Morphology, mountain voles, penile morphology, phylogeny, species delimitation, Yarlung Zangbo River

Introduction

The rich biodiversity of rodents facilitates the identification of new species, and analyses of growing molecular and morphological data reveal their evolutionary relationships (Galewski et al. 2006; Cheng et al. 2017; Liu et al. 2019, 2022; Andreychev and Kuznetsov 2020; Wang et al. 2024). Mountain voles of the genus *Alticola* Blanford, 1881 (Rodentia, Arvicolinae) have a wide distribution in the mountains of Central Asia, living in steppe, rocky montane, and alpine habitats (Hinton 1926; Tang et al. 2018). The genus was first established with *A. stoliczkanus* Blanford, 1875 as the type species. Subsequent research throughout the 19th and 20th centuries led to the description of additional species and subspecies, as well as revisions of their taxonomic ranks based primarily on morphological traits (Hinton 1926; Allen 1940; Ellerman and Morrison-Scott 1951; Gromov and Polyakov 1977). This genus is closely related to *Myodes*, *Craseomys*, and *Eothenomys* according to morphological characteristics, such as palate structure and molars (Hinton 1926; Allen 1940), and molecular phylogenetic

Copyright *Tang, M.K. et al.* This is an open access article distributed under the terms of the Creative Commons Attribution License (CC BY 4.0), which permits unrestricted use, distribution, and reproduction in any medium, provided the original author and source are credited.

analyses (Lebedev et al. 2007; Kohli et al. 2014; Tang et al. 2018). Species of *Alticola* are characterized by pale ash-brown fur and a narrow molar crown. Additionally, the third upper molar (M^3) exhibits a shallow reentrant angle between the first two external angles and an extended posterior lobe (Luo et al. 2000; Smith et al. 2010; Tang et al. 2018). Most taxonomists have recognized *Alticola* as a valid genus (Hinton 1926; Allen 1940; Ellerman and Morrison-Scott 1951; Ognev 1962; Musser and Carleton 1993, 2005; Abramson and Lissovsky 2012; Holden et al. 2017; Wei et al. 2025). According to Musser and Carleton (2005), *Alticola* contains the following 12 species: *A. albicaudus* True, 1894; *A. argentatus* Severtzov, 1879; *A. barakshin* Bannikov, 1947; *A. macrotis* Radde, 1862; *A. semicanus* G. M. Allen, 1924; *A. stoliczkanus*; *A. strelzowi* Kastchenko, 1899; *A. montosa* True, 1894; *A. lemminus* Miller, 1898; *A. olchonensis* Litvinov, 1960; *A. roylei* Gray, 1842; and *A. tuvinicus* Ognev, 1950. The first seven species are distributed in China (Rossolimo et al. 1994; Musser and Carleton 2005; Liu et al. 2020; Wei et al. 2025), with most inhabiting rocky desert environments at high latitudes and elevations. Their occurrence in remote and extreme habitats has resulted in a dearth of comprehensive sampling and systematic research (Bolshakov et al. 2012), a situation that is particularly pronounced for Chinese populations.

The Qinghai-Tibet Plateau's complex topography and climatic history have made it a significant center for rodent diversity, harboring numerous endemic species (Zhang et al. 2022). The Yarlung Zangbo River, which drains its southern region, is a key component of this biodiversity hotspot. Despite this, the river basin remains under-surveyed due to its challenging terrain and poor transportation infrastructure (Wang et al. 2024; Gu and Zhu 2025). For over 20 years, we have collected an extensive series of specimens to investigate phylogenetic relationships within *Alticola* (Tang et al. 2018). Discoveries involved the first documentation of *A. albicauda* from Xinjiang (Liu et al. 2020). In 2008, we collected a morphologically distinctive specimen (Field number GB828002, catalog number SAF 081053) from Lang County, located on the right bank of the middle reaches of the Yarlung Zangbo River in southern Tibet. This specimen was initially identified as *A. stracheyi* by Liu et al. (2012). A subsequent taxonomic revision by Tang et al. (2018) formally synonymized *A. stracheyi* under *A. stoliczkanus*, thereby re-identifying this specimen as *A. stoliczkanus*. Furthermore, Tang et al. (2018) documented at least five distinct molar patterns within *A. stoliczkanus* and reported substantial genetic divergence (K2P distance of 4.3% for *CYTB*) between populations from Lang and Pulan counties. In 2023, we collected eight additional specimens from Lang and Longzi counties morphologically similar to GB828002 and which form a monophyletic clade with it. These collective findings indicate that the identification of these specimens as *A. stoliczkanus* is untenable, leading us to hypothesize that they represent a previously unrecognized species.

To test this hypothesis, we integrate morphological and genetic analyses to determine the taxonomic status of these specimens. Given that the characters of the male genitalia are important in mammalian systematics and provide useful clues to species identification of microtines (Hooper 1958; Hooper and Hart 1962), we evaluate and compare penis morphology among some closely related taxa of *Alticola*. Based on this integrative evidence, we formally describe the population from the Yarlung Zangbo River basin as a new species, *Alticola yarlungia* sp. nov.

Materials and methods

Ethics statement

All specimens were obtained following the American Society of Mammalogists guidelines and the laws and regulations of China concerning the protection of wild terrestrial animals (State Council Order of the People's Republic of China 1992; Sikes and the Animal Care and Use Committee of the American Society of Mammalogists 2016). Field collecting protocols were approved by the Ethics Committee of the Sichuan Academy of Forestry (permit number: SAF2023001). Voucher specimens are deposited at the Sichuan Academy of Forestry (SAF), Chengdu, China.

Sampling and sequencing

Tissue samples for sequencing were collected from across much of the distributional range of the genus *Alticola*, including localities in Russia, Mongolia, Pakistan, Kazakhstan, and northwestern China. In total, 93 specimens were used in our phylogenetic analyses: 42 newly collected and 51 represented by approximately 116 sequences obtained from GenBank. Six specimens, comprising *Neodon irene* and *Volemys millicens*, were included as outgroups to root the phylogeny. Detailed information is provided in Suppl. material 2: appendix 1. The mitochondrial genome sequence of one sample (Field ID: 27253) was aligned using BLASTn against homologous genes from the reference mitogenome of *Alticola stoliczkanus* (XZ16N120), including *CYTB* (GenBank: KY968270), *CO1* (KY968258) and *ND2* (PV614058). We assembled and annotated the mitogenomes from whole-genome shotgun sequencing data for two additional samples (Field ID: 3124 and ZMMU:voucher 4445) using MitoZ v2.3 (Meng et al. 2019) with the --data_size_for_mt_assembly 3,0 parameter.

Total DNA was extracted from 95% alcohol-preserved liver or muscle tissue with the Animal Tissue Genomic DNA Rapid Extraction Kit (Chengdu Fuji Biotechnology Co., Ltd., Sichuan, China). Three mitochondrial genes (mtDNA, cytochrome *b* [*CYTB*, 1,143 bp], cytochrome c oxidase subunit I [*CO1*, 1,545 bp], and NADH dehydrogenase subunit 2 [*ND2*, 1,036 bp]) and four nuclear genes (nuDNA, growth hormone receptor [*GHR*, 883 bp], lecithin cholesterol acyl transferase [*LCAT*, 628 bp], breast

cancer protein 1 [*BRCA1*, 1,022 bp], and interphotoreceptor retinoid-binding protein [*IRBP*, 1,286 bp]) were sequenced for phylogenetic analysis. Primer sets were taken from published literature for *CYTB* (He et al. 2010), *CO1* (Zeng et al. 2013), *ND2* and *IRBP* (Cheng et al. 2017), *GHR* and *LCAT* (Abramson et al. 2009), *BRCA1* (Dubey et al. 2007) (see Suppl. material 1: table S1 for details). The thermal cycling profile was as follows: initial denaturation at 94 °C for 5 min; followed by 40 cycles of denaturation at 94 °C for 45 s, annealing at 49–56 °C for 45 s, and extension at 72 °C for 90 s; with a final extension at 72 °C for 10 min. The PCR products were sequenced at the Sangon Sequencing Center in Chengdu, China. This effort yielded new sequences from five specimens of *Alticola yarlungia* sp. nov. (33 sequences), 64 specimens of *Alticola* (201 sequences), and 24 specimens from *Myodes*, *Craseomys*, *Neodon* and *Volemys* (58 sequences). All these newly generated sequences have been deposited in GenBank, and their corresponding accession numbers are provided in Suppl. material 2: appendix 1.

Phylogenetic analyses and species delimitation

We established three datasets to reconstruct the phylogeny of sequenced individuals as follows: dataset 1 included mtDNA (*CYTB+CO1+ND2*); dataset 2 included nuDNA (*GHR+LCAT+BRCA1+IRBP*); dataset 3 included all mtDNA and nuDNA data. Sequence alignment was initially conducted with MAFFT v7.526 (Katoh and Standley 2013), and conserved regions were subsequently refined using GBLOCKS v0.91b (Castresana 2000) under the -b5 = h parameter. The final lengths of *CYTB*, *CO1*, *ND2*, *GHR*, *LCAT*, *BRCA1*, and *IRBP* used for phylogenetic analyses were 904 bp, 1,545 bp, 1,031 bp, 713 bp, 497 bp, 807 bp, and 1,217 bp, respectively. The Partition Homogeneity (ILD) test implemented in PAUP v4.0a169 using a heuristic search revealed significant incongruence among the three datasets ($p < 0.05$). Based on these results, a concatenated partitioned approach was adopted for phylogenetic trees reconstructions of the three datasets. The optimal model for each gene was identified with PartitionFinder v2.0.0 (Lanfear et al. 2012). The fitness of the model was evaluated using the Akaike information criterion (AIC, Luo et al. 2010). Phylogenetic reconstruction employed Bayesian inference (BI) in MrBayes v3.1.2 and maximum likelihood (ML) in RAxML-NG v1.1.0, with support values from 1,000 bootstrap replicates (Ronquist and Huelsenbeck 2003). The BI analysis was run for 1,000,000 generations with four Markov chain Monte Carlo (MCMC) algorithms (temp = 0.1), sampling every 100 generations, calculating diagnostics every 5,000 generations, and discarding the initial 25% as burn-in. The ML analysis was performed with the parameter --bs-trees 1,000 --brlen linked and using the best-fit models for the seven partitions (Suppl. material 1: table S1).

The average interspecific genetic distannces for *CYTB* were calculated in MEGA v11 (Tamura et al. 2021) using both the Kimura 2-parameter (K2P; Kimura 1980) and the *p*-distance models. Variance was estimated using the bootstrap method with 1,000 replicates. Dataset 3 (mtDNA+nuDNA) was used in the species delimitation analysis. Bayesian species delimitation was performed using the A10 model in BPP v4.8.4 (Yang 2015). A guide tree reconstructed with RAxML-NG served as the phylogenetic framework, employing the JC69 nucleotide substitution model. Two independent MCMC runs were executed, each with 1,000,000 generations and a burn-in of 8,000 generations. A posterior probability threshold of > 0.97 was considered strong support for species boundaries. The Assemble Species by Automatic Partitioning (ASAP) analysis was performed on the online platform: https://bioinfo.mnhn.fr/abi/public/asap/asapold.html (Puillandre et al. 2021) with Kimura (K80) ts/tv 2.0. Multi-rate PTP (mPTP) v0.2.5 was used with the Raxml-ng result of Dataset 3 based on the Maximum-likelihood heuristic method by the --ml --multi parameter (Kapli et al. 2017).

Divergence time estimation

Divergence estimations were calculated using Bayesian evolutionary analysis in BEAST2 v2.7.7 (Bouckaert et al. 2019) on dataset 3. The analysis employed a partitioned framework where substitution models for individual genes were optimized through PartitionFinder2 v2.0.0 (Lanfear et al. 2012), with the selected models subsequently integrated into the BEAUti-generated XML configuration. To accommodate rate heterogeneity, a relaxed log normal molecular clock was applied, while tree topology and node ages were calibrated using a birth-death tree prior to account for potential shifts. The earliest known fossils assigned to each of the following genera were used to set a bound on the age of each group: *Alticola*, 1.5 million years ago (Mya, Serdyuk and Tesakov 2006); *Myodes*, 2.6 Mya (Repenning 1990). Fossil calibrations for *Alticola* (mean = 1.5 Mya, σ = 0.5) and *Myodes* (mean = 2.6 Mya, σ = 0.8) were applied as normal priors, followed by MCMC analysis (500 million generations, sampling every 5,000 steps). After checking convergence (ESS > 200 for all parameters) in Tracer v1.7.2 (Rambaut et al. 2018), the first 25% of generations were discarded as burn-in. The resulting posterior tree distribution was then processed in TreeAnnotator v2.7.4 (Bouckaert et al. 2019) to generate a Maximum Clade Credibility tree, with mean node heights calculated from the post-burn-in samples.

Morphological analyses

Morphological comparisons of *Alticola yarlungia* sp. nov. with congeners distributed in China included 88 adult specimens as follows: nine specimens for *A. yarlungia* sp. nov.,

17 for *A. albicauda*, eight for *A. argentatus*, three for *A. barakshin*, 12 for *A. macrotis*, 15 for *A. semicanus*, 11 for *A. stoliczkanus*, and 13 for *A. strelzowi*. Among these taxa, only *A. yarlungia* sp. nov., and *A. stoliczkanus* occurred in Tibet (Fig. 1). Two individuals of *A. barakshin*, and three individuals of *A. macrotis* were deposited at the Xinjiang Center for Disease Control and Prevention (XJCDC), Xinjiang, China; and two specimens of *A. macrotis* were deposited at the Sichuan Center for Disease Control and Prevention (SCCDC), Chengdu, China. All remaining specimens are deposited at SAF, Chengdu, China (Suppl. material 2: appendix 2).

External, cranial, and dental characteristics were measured for all the specimens. To increase sample sizes, measurable indicators of partial specimens whose skull was damaged were used for statistical analysis. The following external measurements were taken by the collectors in the field on freshly captured specimens and recorded to the nearest 0.1 mm: head body length (HBL), tail length (TL), hind foot length excluding claws (HFL), and ear length (EL). Cranial measurements were taken by Ming Kun Tang and Shao Ying Liu with a Vernier caliper to the nearest 0.01 mm following Yang et al. (2005), Xia et al. (2006) and Tang et al. (2018). Measurements included the skull greatest length (SGL), condylobasal length (CBL), zygomatic breadth (ZB), interorbital breadth (IOB), nasal length (NL), height of braincase (HB), length of maxillary toothrow (LMxT), length of upper molar row (LUMR), width of upper molar rows (M–M), length of lower molar row (LLMR), mandible greatest length (MGL), and mandible length excluding tooth (ML) (Suppl. material 2: appendix 2).

Morphometric analyses were performed using SPSS v19.0. We compiled two datasets from 16 measurements: dataset 1 included *Alticola yarlungia* sp. nov. and the seven other species of *Alticola* distributed in China (*A. albicauda*, *A. argentatus*, *A. barakshin*, *A. macrotis*, *A. semicanus*, *A. stoliczkanus*, and *A. strelzowi*); dataset 2 comprised the three phylogenetically proximate or morphologically similar taxa (*A. yarlungia* sp. nov., *A. stoliczkanus*, and *A. macrotis*). Dataset 1 (n = 67 intact specimens) was subjected to factor analysis (FA) with principal component analysis as the extraction method. Prior to FA, data suitability was confirmed by Kaiser-Meyer-Olkin (KMO = 0.863) and Bartlett's sphericity tests ($P < 0.01$). For dataset 2, we conducted: (1) one-way multivariate analysis of variance (MANOVA) using Pillai's trace statistic to assess overall group differences; (2) one-way analysis of variance (ANOVA) for each measurement; and (3) *post-hoc* comparisons (Tukey's test for equal variances, Tamhane's T2 for unequal variances) between *A. yarlungia* sp. nov. and *A. macrotis*, and *A. yarlungia* sp. nov. and *A. stoliczkanus*.

The glans penis was prepared following the methods of Hooper (1958). Description of baculum followed Liu et al. (2012, 2022). All organs and bacula were illustrated to scale using a camera lucida. Three species' glans penes were prepared, including *Alticola yarlungia* sp. nov., *A. stoliczkanus*, and *A. macrotis*.

Results

Molecular results

The trees resulting from the BI and ML analyses for each dataset had similar topologies and, therefore, only the BI trees were presented here (Figs 2A, 3). The topologies based

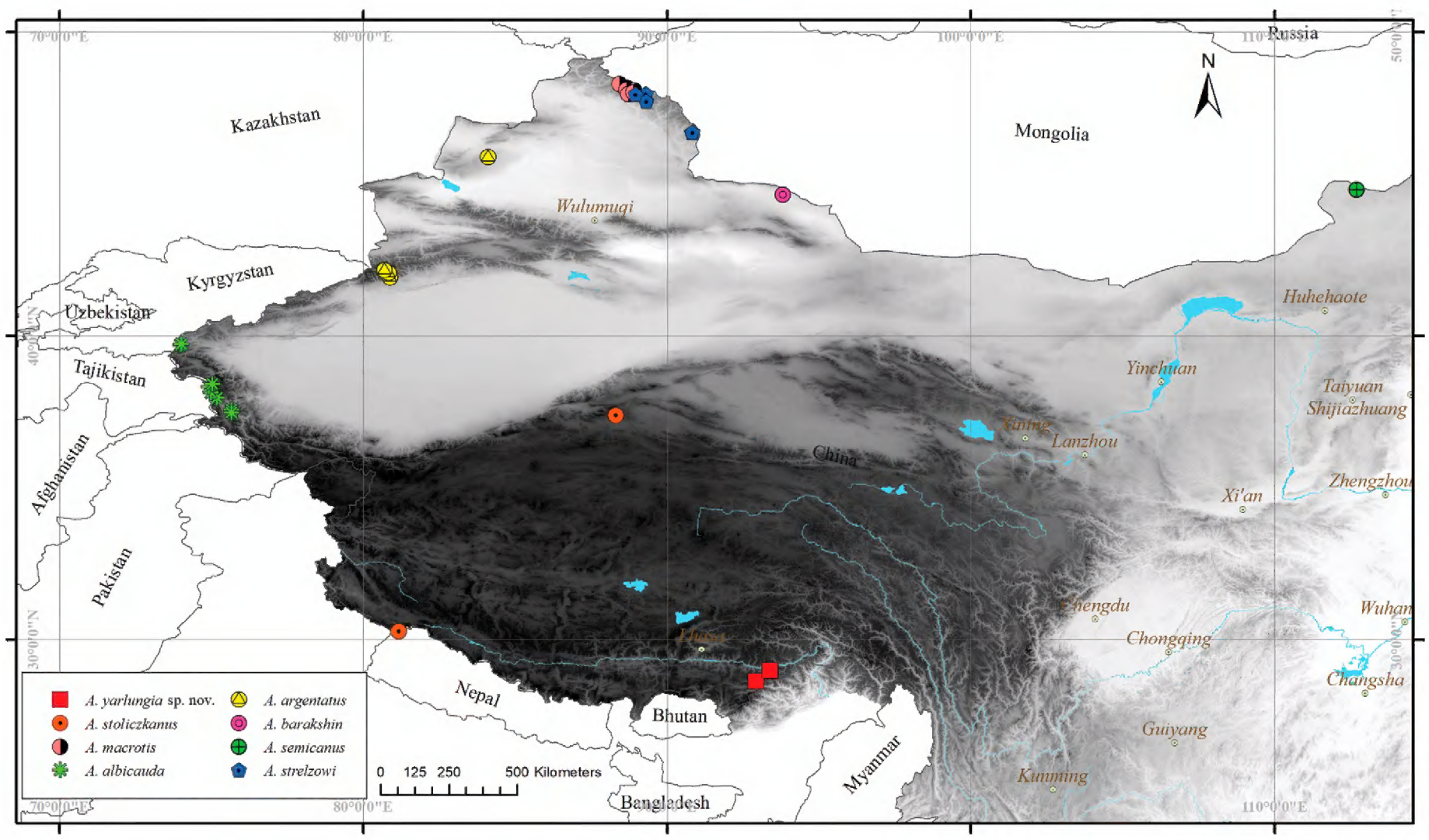

Figure 1. Collection localities of specimens of *Alticola* from China examined in this study.

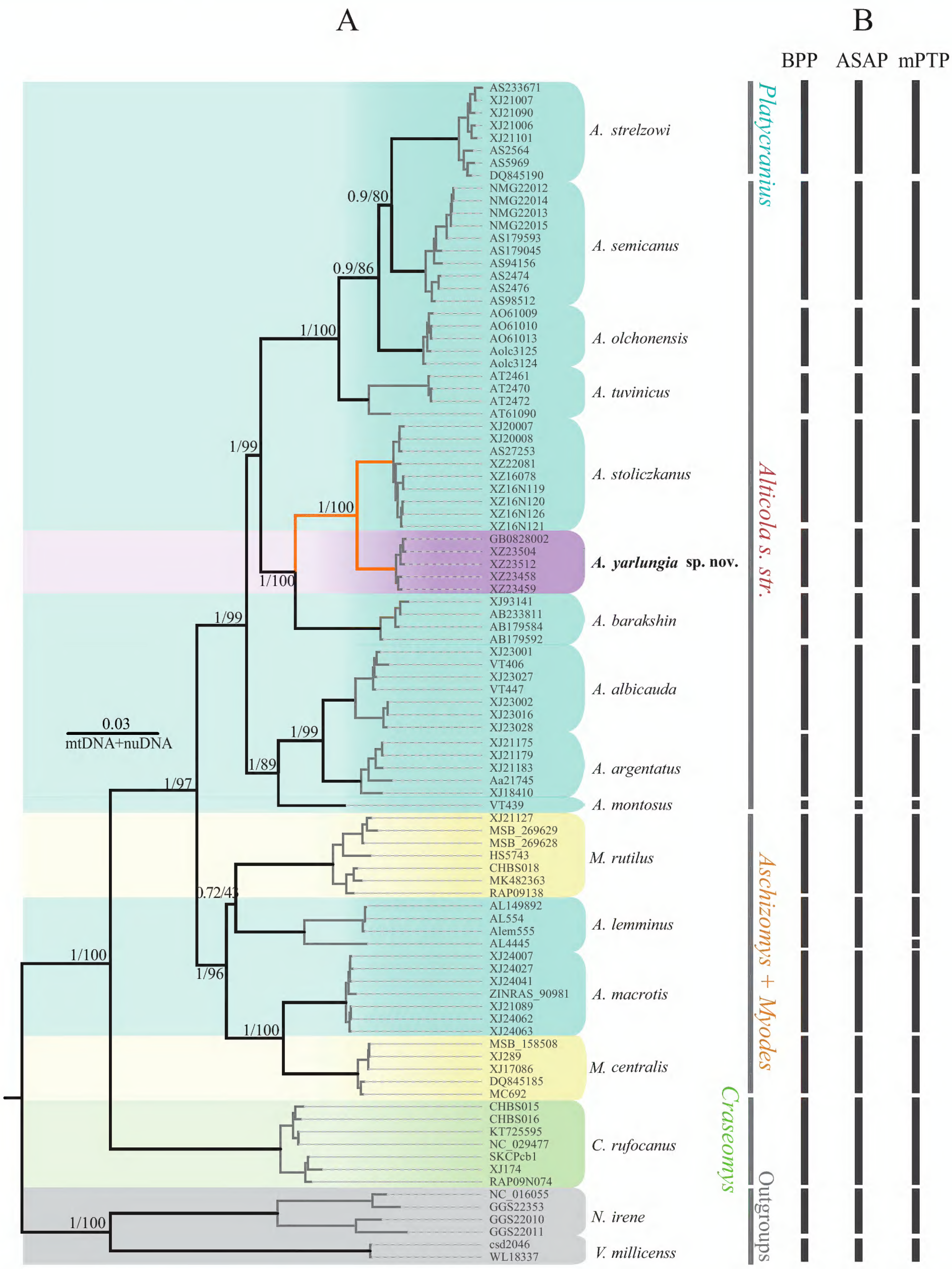

Figure 2. Phylogenetic relationships and species delimitation within *Alticola* and relative genera. **A.** Bayesian inference tree based on concatenated mitochondrial (three genes) and nuclear (four genes) sequences; **B.** Results of species delimitation analysis. Nodal support is indicated as Bayesian posterior probabilities (PP) / maximum likelihood bootstrap percentages (BP). The clade containing *A. yarlungia* sp. nov. is highlighted in orange, indicating its position within the genus and its sister-species relationship (consistent with Figs 3, 4).

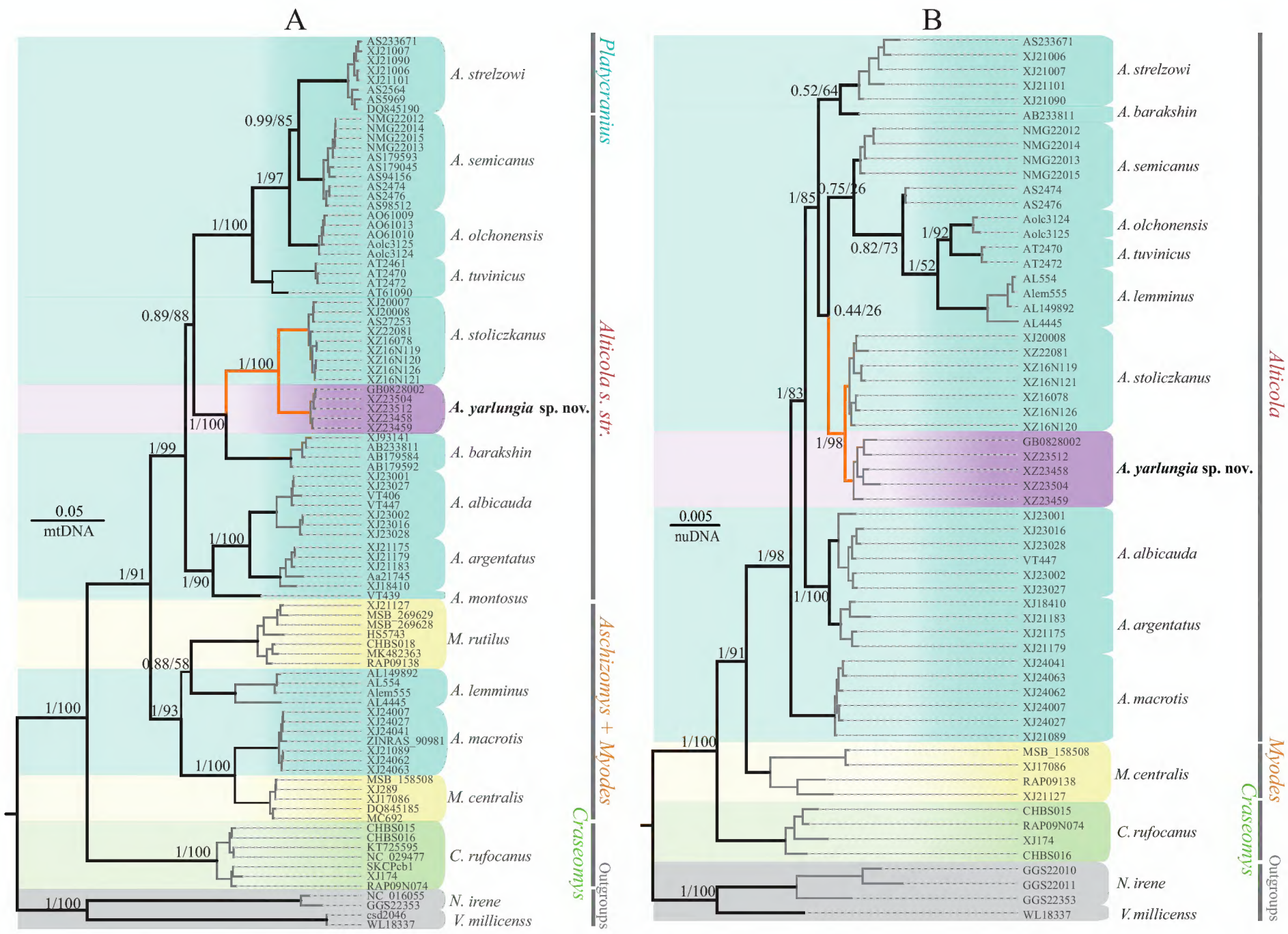

Figure 3. Bayesian phylogenetic trees of *Alticola* and related taxa inferred from **A.** Three concatenated mitochondrial genes and **B.** Four concatenated nuclear genes. Nodal support is indicated as Bayesian posterior probability / maximum likelihood bootstrap percentage (PP/BP).

on datasets 1 and 3 were similar, but these differed from that of dataset 2. Notwithstanding, the five specimens of *Alticola yarlungia* sp. nov. formed a well-supported clade in each tree, and as the sister clade of *A. stoliczkanus* with high Bayesian posterior probability (PP) and bootstrap percentages (BP) values. The BPP, ASAP and mPTP analyses on dataset 3 supported 12, 11 and 14 species within *Alticola*, respectively, with all methods consistently delimiting *A. yarlungia* sp. nov. as an independent lineage (Fig. 2B).

The K2P distances for *CYTB* among *Alticola* taxa ranged from 4.0% to 12.3%, while the *p*-distances ranged from 3.9% to 11.1% (Table 1, Suppl. material 1: table S2). The lowest values were observed between *A. yarlungia* sp. nov. and *A. stoliczkanus*, while the highest were between *A. macrotis* and *A. strelzowi*. The K2P distances (and *p*-distances in parentheses) between *A. yarlungia* sp. nov. and the other 11 species ranged from 4.0% (3.9%) to *A. stoliczkanus* to 10.3% (9.5%) to *A. macrotis*, with an average of 8.1% (Table 1, Suppl. material 1: table S2). BEAST analyses revealed that the divergence between *Alticola* and *Myodes* approximately occurred at approximately 1.76 (95% highest posterior density (HPD) interval = 0.82–2.68)

Table 1. Pairwise estimates of evolutionary divergence between *Alticola* taxa based on *CYTB* sequences, calculated under the K2P model.

Taxon	1	2	3	4	5	6	7	8	9	10	11
1. *yarlungia* **sp. nov.**											
2. *stoliczkanus*	0.040										
3. *macrotis*	0.103	0.108									
4. *albicauda*	0.081	0.093	0.117								
5. *argentatus*	0.082	0.099	0.114	0.050							
6. *barakshin*	0.057	0.062	0.110	0.087	0.083						
7. *semicanus*	0.092	0.105	0.121	0.105	0.105	0.095					
8. *strelzowi*	0.088	0.097	0.123	0.097	0.103	0.087	0.065				
9. *tuvinicus*	0.092	0.103	0.117	0.108	0.106	0.102	0.053	0.065			
10. *montosus*	0.082	0.102	0.095	0.074	0.063	0.079	0.099	0.106	0.102		
11. *olchonensis*	0.084	0.097	0.113	0.097	0.096	0.090	0.045	0.059	0.041	0.093	
12. *lemminus*	0.091	0.098	0.101	0.111	0.108	0.093	0.112	0.112	0.114	0.090	0.105

Mya. The most recent common ancestor of *A. yarlungia* sp. nov. and *A. stoliczkanus* was reconstructed as the phylogenetically youngest divergence node (0.49 Mya, 95% HPD interval = 0.20–0.77), postdating the splits between the clades comprised of *A. strelzowi* and *A. semicanus*, and *A. olchonensis* and *A. tuvinicus* (Fig. 4).

Morphological results

The nine specimens of *Alticola yarlungia* sp. nov. (4 males, 5 females) were all adults, as indicated by complete ossification of the baculum even in the smallest individual (based on HBL). No sexual dimorphism was identified based on skull measurements of the male individual within the range of adult females.

Comparisons of body and skull measurements between *Alticola yarlungia* sp. nov. and seven congeners, along with descriptions of morphological characteristics for all 12 species, were presented in Tables 2, 3, respectively. Side-by-side photographic comparisons of pelages and molars were shown in Figs 5, 6. Morphological comparison of the penis and baculum were shown in Fig. 7. In terms of size, *A. yarlungia* sp. nov. was between *A. macrotis* and *A. argentatus*, being relatively bigger than *A. stoliczkanus* (Table 2). The following four morphological characters separated *A. yarlungia* sp. nov. from its congeners: (1) shortest LUMR and simplest structure of M^3 with a significantly shortened posterior lobe (Fig. 6A1); (2) tail slender and indistinct bicolor, moderate in size, the length about a quarter (24.8%) of the HBL (Fig. 5, Table 3); (3) body dark brown dorsally compared to pale reddish-gray (*A. albicauda*), brownish

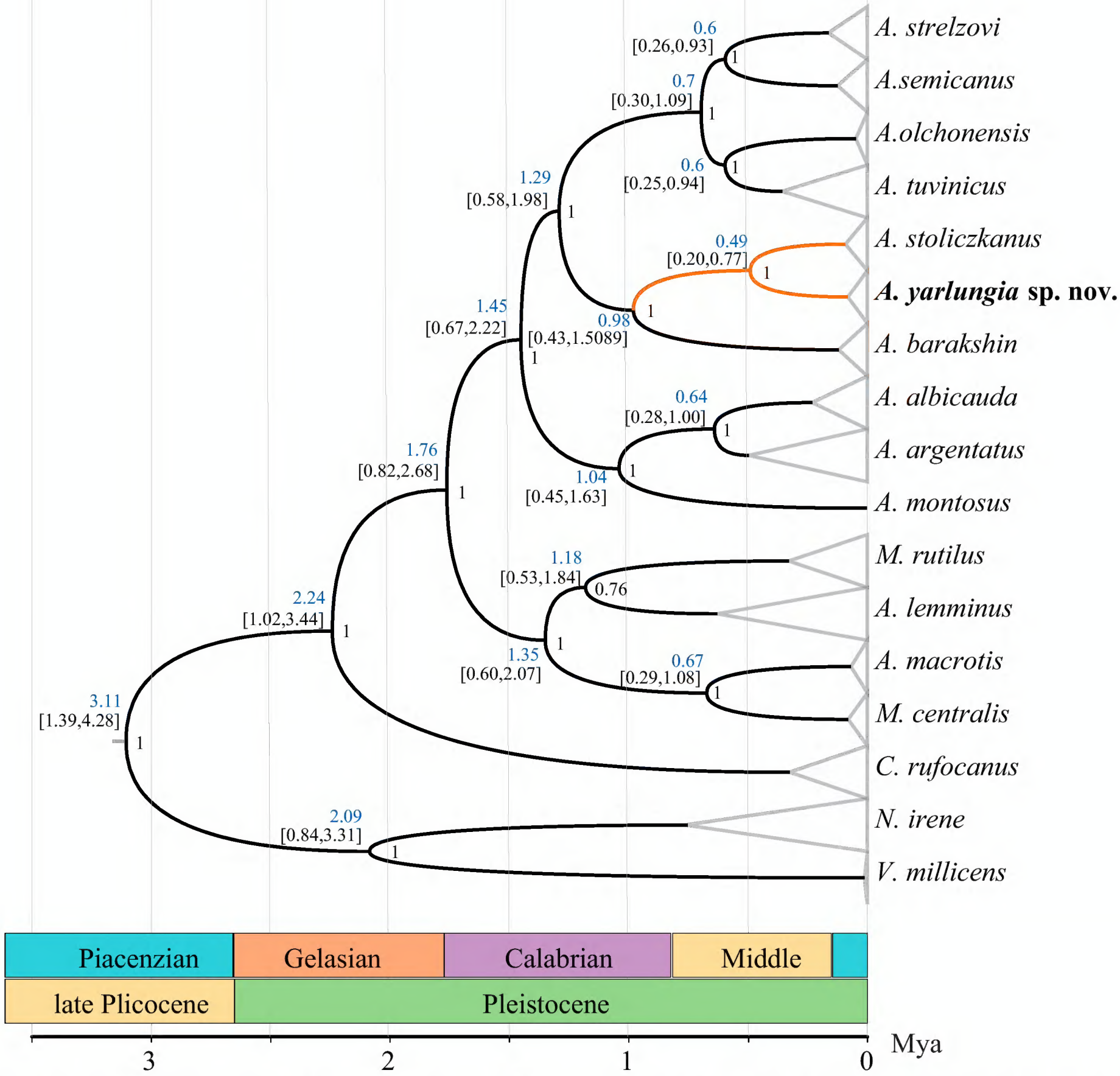

Figure 4. Dated species tree of *Alticola* and related taxa based on three mitochondrial and four nuclear genes, with divergence times estimated using BEAST. Node annotations indicate: left - mean divergence times (blue; Mya) and 95% HPD interval (black; in square brackets); right - PP values (black).

Table 2. External and cranial measurements (mm) of eight taxa of *Alticola* from China (Mean ± SD (range; n = number of specimens); for abbreviations see Materials and methods).

Measurement	Holotype	*A. yarlungia* sp. nov.	*A. stoliczkanus*	*A. macrotis*	*A. albicauda*	*A.argentatus*	*A. barakshin*	*A. semicanus*	*A. strelzowi*
HBL	104	102.00 ± 5.90 (92~110; n = 9)	91.91 ± 3.91 (85~98; n = 11)	96.74 ± 3.60 (88~101.4; n = 12)	104.94 ± 7.91 (92~120; n = 17)	102.25 ± 6.04 (94~111; n = 8)	111.67 ± 11.93 (102~125; n = 3)	110.8 ± 7.87 (100~128; n = 15)	104.38 ± 9.36 (90~124; n = 13)
TL	24	25.22 ± 1.79 (23~28; n = 9)	20.09 ± 1.87 (17~23; n = 11)	29.76 ± 2.80 (27~36; n = 12)	45.32 ± 4.7 (39~55; n = 17)	39.63 ± 5.32 (33~47; n = 8)	23 ± 1 (22~24; n = 3)	34 ± 2.14 (30~37; n = 15)	41.31 ± 4.73 (35~50; n = 13)
HFL	18	17.78 ± 0.67 (17~19; n = 9)	16.91 ± 0.83 (15~18; n = 11)	17.74 ± 0.57 (17~18.6; n = 12)	18.09 ± 1.18 (16~20; n = 17)	18.5 ± 1.2 (17~20; n = 8)	18.67 ± 1.53 (17~20; n = 3)	20.87 ± 0.92 (20~23; n = 15)	19.31 ± 0.75 (18~20; n = 13)
EL	12	14.44 ± 1.24 (12~16; n = 9)	12.82 ± 0.4 (12~13; n = 11)	14.32 ± 0.81 (13~16; n = 12)	15.41 ± 0.87 (14~17; n = 17)	15.13 ± 0.64 (14~16; n = 8)	15.67 ± 1.15 (15~17; n = 3)	15.27 ± 0.96 (13~17; n = 15)	17.54 ± 1.13 (16~20; n = 13)
SGL	24.77	25.03 ± 0.99 (23.43~26.2; n = 7)	25.18 ± 1.15 (23.46~27.01; n = 11)	25.29 ± 0.81 (23.9~26.21; n = 8)	26.33 ± 0.79 (25.03~27.96; n = 17)	26.48 ± 0.75 (25.75~27.86; n = 6)	28.13 ± 1.63 (27~30; n = 3)	28.4 ± 0.84 (27.5~29.84; n = 13)	27.09 ± 1.47 (24.87~29.11; n = 9)
CBL	22.76	22.9 ± 1.00 (21.23~24.02; n = 7)	22.77 ± 1.17 (21.06~24.46; n = 11)	22.72 ± 1.07 (21.25~24.5; n = 8)	23.93 ± 0.93 (22.57~25.45; n = 17)	23.84 ± 0.83 (22.98~25.29; n = 6)	25.98 ± 1.74 (24.87~27.98; n = 3)	25.57 ± 1.02 (24.42~27.55; n = 13)	24.58 ± 1.3 (22.39~26.34; n = 9)
ZB	13.35	13.53 ± 0.95 (11.71~14.88; n = 9)	13.14 ± 0.63 (12.25~14.04; n = 11)	13.38 ± 0.57 (12.5~14.1; n = 8)	13.8 ± 0.94 (12.62~15.38; n = 17)	14.03 ± 0.55 (13.51~14.99; n = 6)	15.2 ± 0.75 (14.5~16; n = 3)	14.91 ± 0.8 (13.87~16.44; n = 14)	14.57 ± 1.09 (13.4~16.22; n = 9)
IOB	3.84	4.07 ± 0.15 (3.84~4.33; n = 9)	4.11 ± 0.23 (3.78~4.49; n = 11)	3.94 ± 0.17 (3.72~4.16; n = 9)	4.03 ± 0.2 (3.74~4.41; n = 17)	4.22 ± 0.2 (3.94~4.47; n = 6)	4.07 ± 0.06 (4~4.1; n = 3)	4.29 ± 0.15 (4.07~4.57; n = 14)	4.53 ± 0.23 (4.3~5; n = 9)
NL	7.49	7.66 ± 0.47 (7.05~8.34; n = 9)	7.73 ± 0.6 (6.87~8.58; n = 10)	6.81 ± 0.44 (6.09~7.25; n = 6)	8 ± 0.36 (7.55~8.98; n = 16)	8.04 ± 0.49 (7.59~8.93; n = 6)	8.68 ± 0.55 (8.34~9.32; n = 3)	8.67 ± 0.43 (8.2~9.42; n = 13)	7.71 ± 0.77 (6.75~8.86; n = 8)
HB	9.06	9.15 ± 0.37 (8.66~9.62; n = 7)	9.64 ± 0.32 (9.24~10.33; n = 11)	9.33 ± 0.45 (8.67~10.14; n = 9)	9.74 ± 0.4 (9.2~10.3; n = 17)	9.83 ± 0.29 (9.56~10.35; n = 6)	10.82 ± 0.4 (10.55~11.28; n = 3)	10.18 ± 0.3 (9.72~10.76; n = 14)	7.87 ± 0.33 (7.17~8.25; n = 9)
M–M	4.81	5.13 ± 0.16 (4.81~5.37; n = 9)	5.11 ± 0.27 (4.81~5.61; n = 11)	5.06 ± 0.17 (4.84~5.27; n = 6)	5.11 ± 0.18 (4.88~5.46; n = 16)	5.16 ± 0.23 (4.85~5.48; n = 6)	5.66 ± 0.33 (5.46~6.04; n = 3)	5.55 ± 0.2 (5.26~5.9; n = 13)	5.1 ± 0.25 (4.64~5.49; n = 8)
LMxT	14.44	14.78 ± 0.59 (13.83~15.54; n = 9)	14.64 ± 0.81 (13.57~15.99; n = 11)	14.08 ± 0.39 (13.57~14.54; n = 6)	15.37 ± 0.89 (14.47~17.74; n = 16)	15.35 ± 0.6 (14.68~16.15; n = 7)	16.2 ± 0.71 (15.74~17.02; n = 3)	15.98 ± 0.61 (15.3~17.09; n = 13)	14.8 ± 0.9 (13.77~16.28; n = 8)
LUMR	5.12	5.58 ± 0.24 (5.12~5.85; n = 9)	5.53 ± 0.2 (5.31~5.82; n = 11)	5.60 ± 0.16 (5.43~5.86; n = 9)	5.81 ± 0.3 (5.46~6.48; n = 17)	5.72 ± 0.23 (5.49~6.13; n = 7)	5.79 ± 0.31 (5.56~6.14; n = 3)	6.07 ± 0.29 (5.71~6.52; n = 14)	5.6 ± 0.27 (5.2~6.17; n = 9)
LLMR	5.29	5.57 ± 0.23 (5.29~6.05; n = 9)	5.53 ± 0.32 (5.14~6.1; n = 11)	5.29 ± 0.35 (4.48~5.62; n = 9)	5.81 ± 0.29 (5.42~6.4; n = 17)	5.67 ± 0.14 (5.43~5.91; n = 8)	5.82 ± 0.34 (5.61~6.22; n = 3)	6.1 ± 0.31 (5.74~6.68; n = 14)	5.34 ± 0.24 (4.89~5.76; n = 9)
MGL	17.35	17.63 ± 0.84 (16~18.54; n = 9)	17.7 ± 1.07 (15.95~19.55; n = 11)	17.54 ± 0.60 (16.79~18.37; n = 9)	18.26 ± 0.84 (17.29~19.64; n = 17)	18.2 ± 0.47 (17.7~18.96; n = 8)	20.02 ± 1.23 (19.28~21.44; n = 3)	19.27 ± 0.74 (18.27~20.56; n = 14)	17.84 ± 0.91 (16.67~19.01; n = 9)
ML	14.52	14.87 ± 1.02 (13.07~16.33; n = 9)	15.4 ± 0.85 (14.05~16.58; n = 11)	14.84 ± 0.23 (14.48~15.19; n = 6)	15.71 ± 0.63 (14.87~16.62; n = 16)	15.59 ± 0.59 (14.9~16.64; n = 8)	17.03 ± 1.2 (16.33~18.42; n = 3)	16.89 ± 0.58 (16.16~17.94; n = 13)	15.47 ± 0.73 (14.59~16.55; n = 8)

Note: Sample sizes (n) vary for some measurements due to damage or incomplete preparation of specimens.

gray (*A.argentatus*, *A. barakshin*), and gray (*A. semicanus*, *A. strelzowi*) in other species (Table 3); (4) glans and bacula morphology of *A. yarlungia* sp. nov. differed from *A. stoliczkanus* and *A. macrotis* as follows: outer crater papillae (Fig. 7b), shape of proximal bacula (Fig. 7m), distal bacula (Fig. 7a), and lateral bacula (Fig. 7k), urethral lappet (Fig. 7A3, B3, C3), and dorsal papillae (Fig. 7A4, B4, C4).

As shown in Table 4, the first three factors with eigenvalues greater than 1.0 (9.604, 2.178, and 1.103) collectively explained 80.53% of the total variance. The first factor (Factor 1) accounted for 60.02% of the total original variance and most variables (but not TL, HFL, EL, and IOB) had high positive loadings, suggesting that it related to size variation. The second factor (Factor 2) explained 13.62% of the total variance and it was positively correlated with TL and EL with factor loadings 0.882 and 0.759, respectively. Factor 3 accounted for 6.90% of the total variance, the main morphological variable was IOB, with relatively higher factor loading (0.885). In scatterplot, specimens of *A. yarlungia* sp. nov. and *A. macrotis* overlapped heavily at the center of the scatterplot, but separating from the specimens of other six species distinctly. Some specimens of *A. stoliczkanus* plotted near to the morphospace occupied by *A. yarlungia* sp. nov. and *A. macrotis*, suggesting that they have relatively similar body proportions and skull characteristics (Fig. 8). This result was consistent with the molecular phylogenetic trees (Figs 2–4).

The one-way MANOVA performed on morphometric dataset 2 obtained a significant difference among *Alticola yarlungia* sp. nov., *A. stoliczkanus*, and *A. macrotis* (Pillai's trace = 1.925, F = 7.985, df = 32, error df = 10, $P < 0.01$). The ANOVA result also obtained significant differences between the three taxa for HBL, TL, HFL, EL, NL, and HB (Suppl. material 1: table S3). Further, Tukey's (or Tamhane's T2) *post-hoc* tests revealed statistically significant differences in HBL, TL, HFL, EL, and HB between *A. yarlungia* sp. nov. and *A. stoliczkanus*.

Table 3. Morphological characteristics comparison between *Alticola yarlungia* sp. nov. and 12 congeners.

Species	Body	Tail	Skull and Molar
***A. yarlungia* sp. nov.**	Dorsum dark brown, sides and venter gray with pure white tips, sharply demarcated.	Tail relatively short and slender, sparsely haired (mean TL/HBL ratio 24.8%); indistinctly bicolored, light brown dorsally and gray white ventrally, with a terminal tuft approximately 7 mm long.	Skull smallest in size. LUMR is the shortest. M^3 is the simplest, characterized by a significantly shortened posterior lobe. It exhibits two lingual reentrant folds creating two well-developed angles, with the posterior lobe itself forming a third lingual angle. On the labial side, there are three angles; the first labial reentrant is very shallow, while the second is broad and deep.
A. stoliczkanus*	Tibetan specimens: dorsum bright ferruginous brown, venter white, the two colors sharply divided. Xinjiang specimens: dorsum dull pale brown.	Tail shortest (mean TL/HBL ratio 21.9%); covered with stiff fulvescent-white hair, extending approximately 13 mm beyond the tail tip.	Skull smallest in size. M^3 reduced, with three labial and two lingual salient angles, and a slight trace of a fourth labial angle and a third lingual angle behind; the second labial reentrant is very wide, and the second lingual reentrant always shallow or absent; the posterior lobe is less than half of M^3.
A. macrotis*	Dorsum generally dark brownish-gray; sides and venter gray, hairs tipped with pure white, coloration sharply demarcated.	Tail relatively short (mean TL/HBL ratio 30.8%); distinctly bicolored, dark brown dorsally and whitish ventrally, with a distinct short hairy tip.	Skull smallest in size. Depth of the first external reentrant angles of M^3 is close to that of the second, occasionally almost as deep; M^3 with three labial salient angles (occasionally a rudimentary fourth) and three lingual salient angles; posterior lobe of M^3 usually points straight back; the surface of M^3 typically exhibits only one closed space, with the second being nearly separate in some specimens occasionally with almost separated second. M_1 has six closed fields, of which the first is occasionally incompletely separated from second.
A. albicauda*	Pale reddish-gray dorsally, venter hairs pure white with gray bases.	Tail longest (mean TL/HBL ratio 43.2%); uniformly pure white, ending in a terminal tuft approximately 12 mm long.	Skull moderate in size. LUMR longer; there are three outer and three inner salient angles in M^3; the third labial reentrant fold is so reduced that the third triangle is rather broadly confluent with the posterior loop.
A.argentatus*	Dorsum a variable mixture of fawn-brown and gray tones, venter grayish to dirty-white, evenly demarcated from the sides.	Tail moderate in length (mean TL/HBL ratio 38.7%); usually uniformly pale, but occasionally inconspicuously bicolored (dorsum light brown or straw-gray, venter pale).	Skull relatively flat and moderate in size, with rather short orbit. M^3 usually compressed anteriorly (with a narrow second labial infold) and possesses an elongated posterior loop; the third lingual angle is consistently well-developed and pointed.
A. barakshin*	Brownish-gray with dull rusty tone dorsally, venter dirty white.	Tail shorter (mean TL/HBL ratio 20.8%); indistinct bicolored, light sandy-brownish dorsally and buffy white ventrally.	Skull largest in size. M^3 structurally simple, with only two lingual and three labial salient angles; the posterior lobe constitutes approximately half the tooth's length.
A. semicanus*	Dorsum brownish mouse gray, venter buffy white, with dark based hairs.	Tail relatively short (mean TL/HBL ratio 30.8%); uniformly buffy white with a terminal tuft, in some individuals the dorsum is light brown.	Skull largest in size, angular and relatively flat. LUMR longest. M^3 with three well-developed salient angles per side; its posterior loop shut off from the third triangle, rather long, with variable vestigial traces of fourth/fifth labial and fourth lingual angles. Enamel of M_3 has four loops.
A. strelzowi*	Dorsum ashy gray, irregularly brightened by the yellowish or slightly rufous subterminal bands on the hairs; venter white, irregularly darkened by the slate-colored bases of the hairs.	Tail moderate in length (mean TL/HBL ratio 39.6%); uniformly white or cream, occasionally slightly darker above (cream-buff) than below (cream-white).	Skull larger in size, remarkably broad and flat, HB approximately half of ZB. M^3 much simplified with three salient angles on each side, the first outer triangle small and broadly confluent with the anterior loop.
A. montosa (True 1894; Hinton 1926)	Dorsum dull grayish brown; venter silvery gray, darkened by slate bases of fur and without buffy suffusion.	Tail longer (mean TL/HBL ratio ≈33% or more); bicolored, dusky above and whitish below; terminal tuft very short.	Skull rather longer, narrower and flatter than in *A. roylei*; auditory bullae considerably larger. M^3 with four labial and three lingual angles; M_1 with four labial and four lingual angles, its first labial angle as long as the subsequent ones. In M_3, the middle labial and lingual angles alternate, creating a non-lozenge-shaped space between them.
A. lemminus (Bodrov et al. 2016; Holden et al. 2017)	Dorsum ash gray washed with brown, venter whitish gray, and flank demarcation distinct.	Tail shortest, TL/HBL ratio about 16–24%; distinctly bicolored, blackish brown above and gray below, with a distinct tuft.	Skull small, semicircular, and delicate. Molars resemble those of *Myodes* rather than *Alticola*. On M^3, the first labial reentrant fold is distinctly deeper, enamel is thick, cement accumulation is modest, and angles are rounded. M^3 has four salient angles on each side.
A. olchonensis (Bodrov et al. 2016; Holden et al. 2017)	Dorsum gray and washed brown, venter whitish with buffy shades.	Tail relatively short (27–32% of HBL); bicolored and densely haired, with a distinct terminal tuft.	Skull closely resembles the more widespread *A. tuvinicus*. M^3 with three or four lingual angles and three labial angles; the second labial reentrant fold usually wide.
A. roylei (Hinton 1926)	Dorsum rich dark brown, venter gray, darkened by slate-based hairs, with no sharp demarcation from the dorsum.	Tail moderate in length (TL/HBL ratio 33–36%); sharply bicolored, dark brown above and grayish-white below.	Skull strongly built, with ZB sometimes exceeding 60% of CBL; auditory bullae small and rounded. Cheek teeth robust. M^3 with at least three salient angles on each side; the third lingual angle is always well developed, often showing vestiges of a fourth angle on the lingual, labial, or both sides. M_1 with four labial and five lingual salient angles.
A. tuvinicus (Rossolimo et al. 1994; Bodrov et al. 2016; Holden et al. 2017)	Dorsum generally dull ash-gray, often with brown tones, venter typically grayish-pale. The flank demarcation is usually straight.	Tail longer (TL/HBL ratio 32–46%); sharply or gradually bicolored, with the dorsal color typically matching the tone of the back.	Skull large; braincase rather flattened (though less so than in *A. semicanus*). M^3 long, typically with a fully developed posterior loop (occasionally somewhat shortened); it bears three lingual and three labial angles, the third lingual angle consistently large and pointed; the second labial reentrant fold is usually wide.

Note: An asterisk (*) denotes species of *Alticola* present in China that were directly examined in this study. Species without an asterisk are not considered to occur in China; their morphological characteristics are summarized from literature records (see References).

Also, *A. yarlungia* sp. nov. and *A. macrotis* differed significantly in HBL, TL, and NL (Suppl. material 1: table S3).

The glans penis morphology of *Alticola yarlungia* sp. nov. exhibited distinct differences in outer crater papillae, proximal, distal and lateral bacula, urethral lappet, and dorsal papillae with *A. stoliczkanus* and *A. macrotis* (Fig. 7). It had 4–5 outer crater papillae each side, whereas *A. stoliczkanus* had only one, and *A. macrotis* lacked them entirely (Fig. 7b). The base of the proximal baculum was semicircular shape in *A. yarlungia* sp. nov., while it was slightly enlarged in *A. stoliczkanus* and *A. macrotis* (Fig. 7m). In *A. yarlungia* sp. nov., the distal and lateral bacula were slender, and the lateral bacula possessed a sharp tip, distinguishing them from those of *A. stoliczkanus* and *A. macrotis* (Fig. 7a, k).

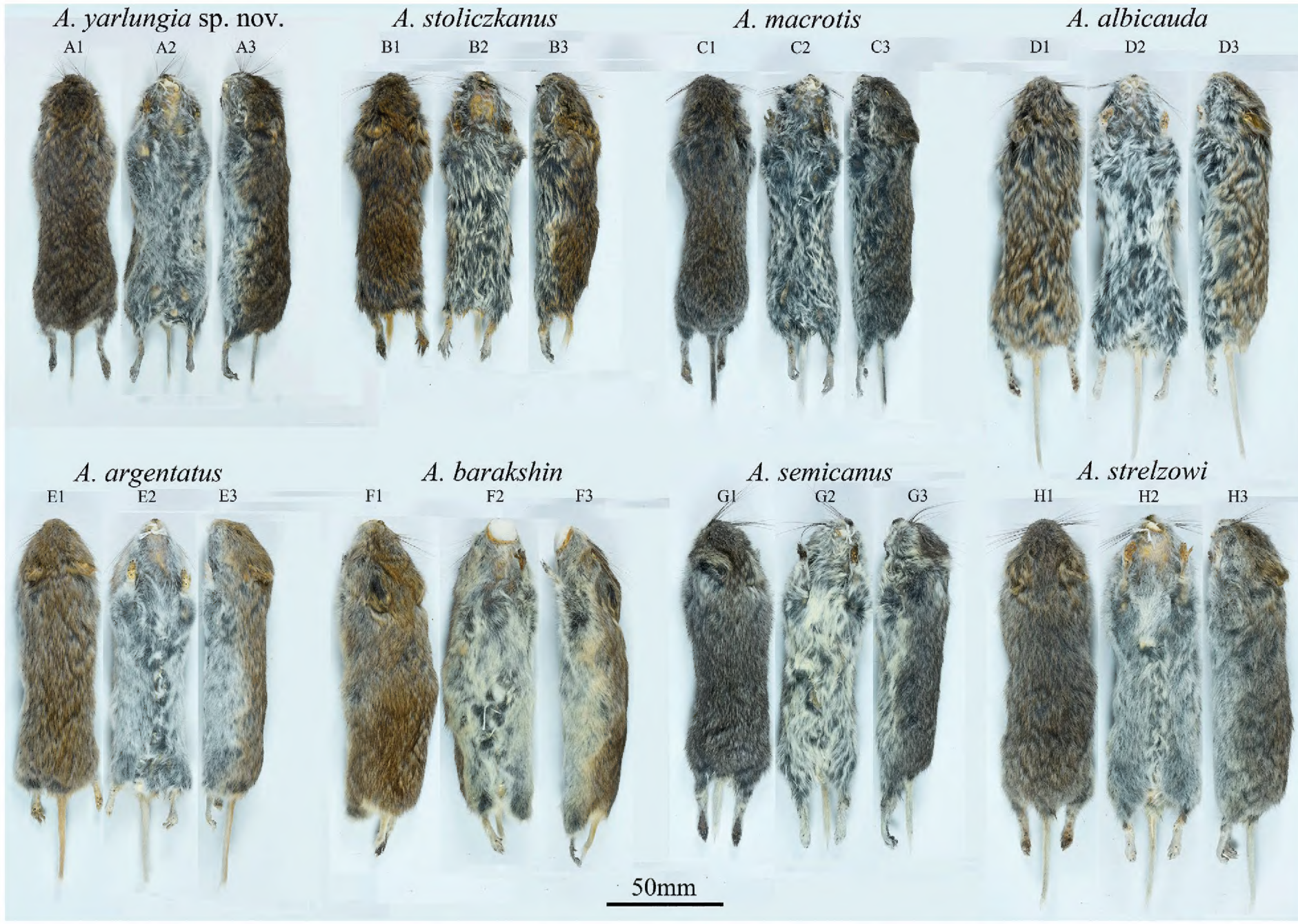

Figure 5. Pelage comparison of *Alticola*. *A. yarlungia* sp. nov. (**A.** Voucher XZ23458), *A. stoliczkanus* (**B.** XZ16120), *A. macrotis* (**C.** XJ24041), *A. albicauda* (**D.** XJ23002), *A. argentatus* (**E.** XJ21175), *A. barakshin* (**F.** SWUN93141), *A. semicanus* (**G.** NMG22012), and *A. strelzowi* (**H.** XJ21008). Images show dorsal (1), ventral (2), and lateral (3) views.

Table 4. Factor loadings and variance explained from factor analysis of morphometric data for *Alticola* taxa distributed in China.

Variables	Factor component		
	1	2	3
HBL	0.669	0.525	0.208
TL	0.178	0.882	-0.057
HFL	0.430	0.333	0.498
EL	-0.026	0.759	0.429
SGL	0.808	0.299	0.460
CBL	0.823	0.303	0.431
ZB	0.743	0.346	0.434
IOB	0.125	0.076	0.885
NL	0.833	0.103	0.267
HB	0.759	-0.355	-0.295
M–M	0.740	-0.151	0.347
LMxT	0.862	0.197	0.162
LUMR	0.789	0.326	-0.004
LLMR	0.907	0.124	-0.060
MGL	0.895	0.082	0.279
ML	0.923	0.120	0.210
Eigenvalues	9.604	2.178	1.103
Variance explained (%)	60.023	13.615	6.895

The urethral lappet had two long forks, with deep bifurcation in *A. yarlungia* sp. nov., whereas *A. stoliczkanus* had two short forks and *A. macrotis* had three forks (Fig. 7A3, B3, C3). The dorsal papilla with a distalis digitation in *A. yarlungia* sp. nov., which was significantly different from *A. stoliczkanus* and *A. macrotis* (Fig. 7A4, B4, C4).

Discussion

The genus *Alticola* exhibits characteristics suggestive of convergent or parallel morphological evolution and relatively recent diversification (Lebedev et al. 2007). The divergence time between *Alticola* and its closest sister group, *Myodes*, is roughly 2 Mya (Kohli et al. 2014). Some species pairs of *Alticola*, such as *A. argentatus* and *A. albicauda*, appear to have diverged from each other around 0.5 Mya. The divergence time is very recent and with relatively low uncorrected *p*-distances 3.8% (Kohli et al. 2014). The topology of our reconstructed phylogenetic tree for *Alticola* largely aligns with previous studies (Kohli et al. 2014, Bodrov et al. 2016; Tang et al. 2018). Furthermore, our phylogenetic analyses consistently recognize *A. yarlungia* sp. nov. as a sister clade of *A. stoliczkanus* within subgenus *Alticola sensu stricto* (*s. str.*) (Figs 2–4). The K2P and *p*-distance of *CYTB* between *A. yarlungia* sp. nov. and *A. stoliczkanus* is 4.0% and 3.9% respectively (Table 1), and the divergence time between them is roughly 0.49 Mya (95% HPD interval: 0.20–0.77; Fig. 4). The specimens of *A. stoliczkanus* collected from four distant sites (Pulan, Ritu and Jilong counties, Tibet, and Ruoqiang County, Xinjiang) clustered in a supported clade (Figs 2, 3), and have an intraspecific genetic distance of 0.53%. These results indicate that *A. stoliczkanus* has a relatively lower intraspecific genetic

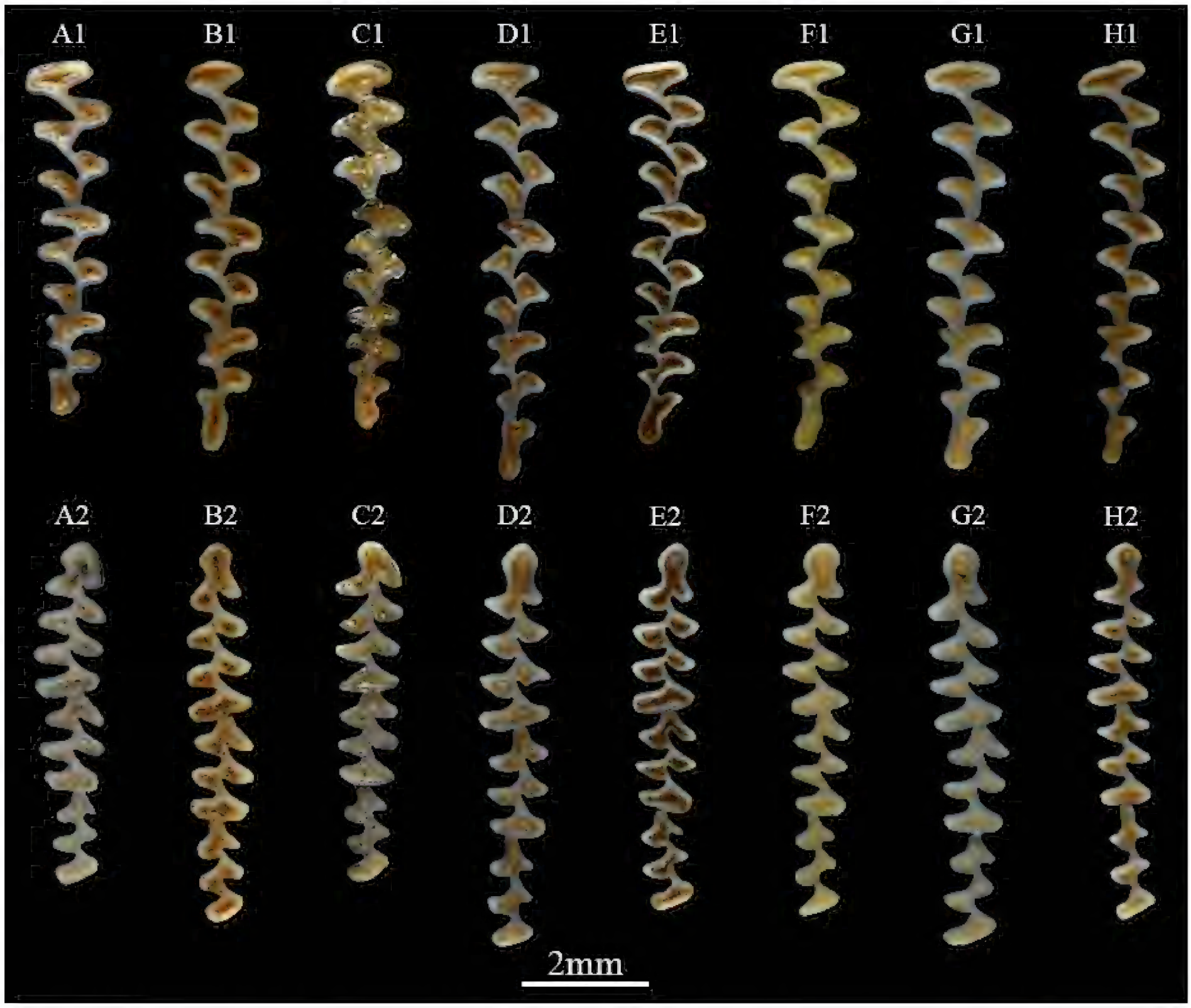

Figure 6. Molar comparison of *Alticola* occurring in China (species and voucher numbers correspond to Fig. 5). Images show the right upper (1) and right lower (2) molar rows.

distance between different populations, and despite its broad distribution. The nine specimens of *A. yarlungia* sp. nov. were collected from the middle-lower reaches of the Yarlung Zangbo River in Lang and Longzi counties, Tibet. Despite the geographic proximity of these sample sites to those of *A. stoliczkanus* (in Jilong and Pulan counties), the two taxa exhibit substantial genetic divergence (K2P = 4.0%). Meanwhile, some other species pairs of *Alticola* that differentiated later have relatively low *CYTB* genetic distances (Fig. 4). For instance, the K2P distances (and *p*-distances in parentheses) among *A. olchonensis* and *A. tuvinicus*, *A. olchonensis* and *A. semicanus*, and *A. argentatus* and *A. albicauda* are 4.1% (4.0%), 4.5% (4.3%) and 4.7% (4.5%), respectively (Table 1, Suppl. material 1: table S2). These results closely match those reported by Bodrov et al. (2016). Accordingly, the reconstructed phylogenetic tree and relatively high genetic distances support the recognition of *A. yarlungia* as a distinct species that arose from a recent divergence.

Morphological evidence also supports the validity of *Alticola yarlungia* sp. nov. Hinton (1926) and Tang et al. (2018) pointed out that the M^3 pattern easily discriminates closely related species of *Alticola*, *Myodes*, and *Craseomys*. Further, *Alticola* generally differs from *Myodes* and *Craseomys* in having a shallow reentrant angle between the first two external angles, an extended posterior lobe, and a simpler structure of M^3, as well as by pale ash-brown fur (Luo et al. 2000; Smith et al. 2010; Tang et al. 2018). The structure of M^3 also well-discriminates the species of *Alticola* (Hinton 1926; Ognev 1962; Gromov and Polyakov 1977; Bodrov et al. 2016; Kryštufek et al. 2017; Tang et al. 2018). Our factor analysis reveals that 16 morphometric indexes unambiguously distinguished *A. yarlungia* sp. nov. from the other six congeners occurring in China, except for *A. macrotis* (Fig. 8). The length and darker dorsal color of tail (Fig. 5), the ratio of TL to HBL (average 30.8% vs. 24.8%, Table 3), the deeper first labial reentrant, the more robust third inner angle and extended posterior loop of M^3 (Fig. 6; Bolshakov et al. 2012), and their distributions (Luo et al. 2000) usually distinguish *A. macrotis* from *A. yarlungia* sp. nov. In appearance, *A. yarlungia* sp. nov. differs from congeners by the color of body and tail (Fig. 5, Table 3). *Alticola stoliczkanus* was described based on the type specimen collected in Ladakh. It is the most widely distributed species of

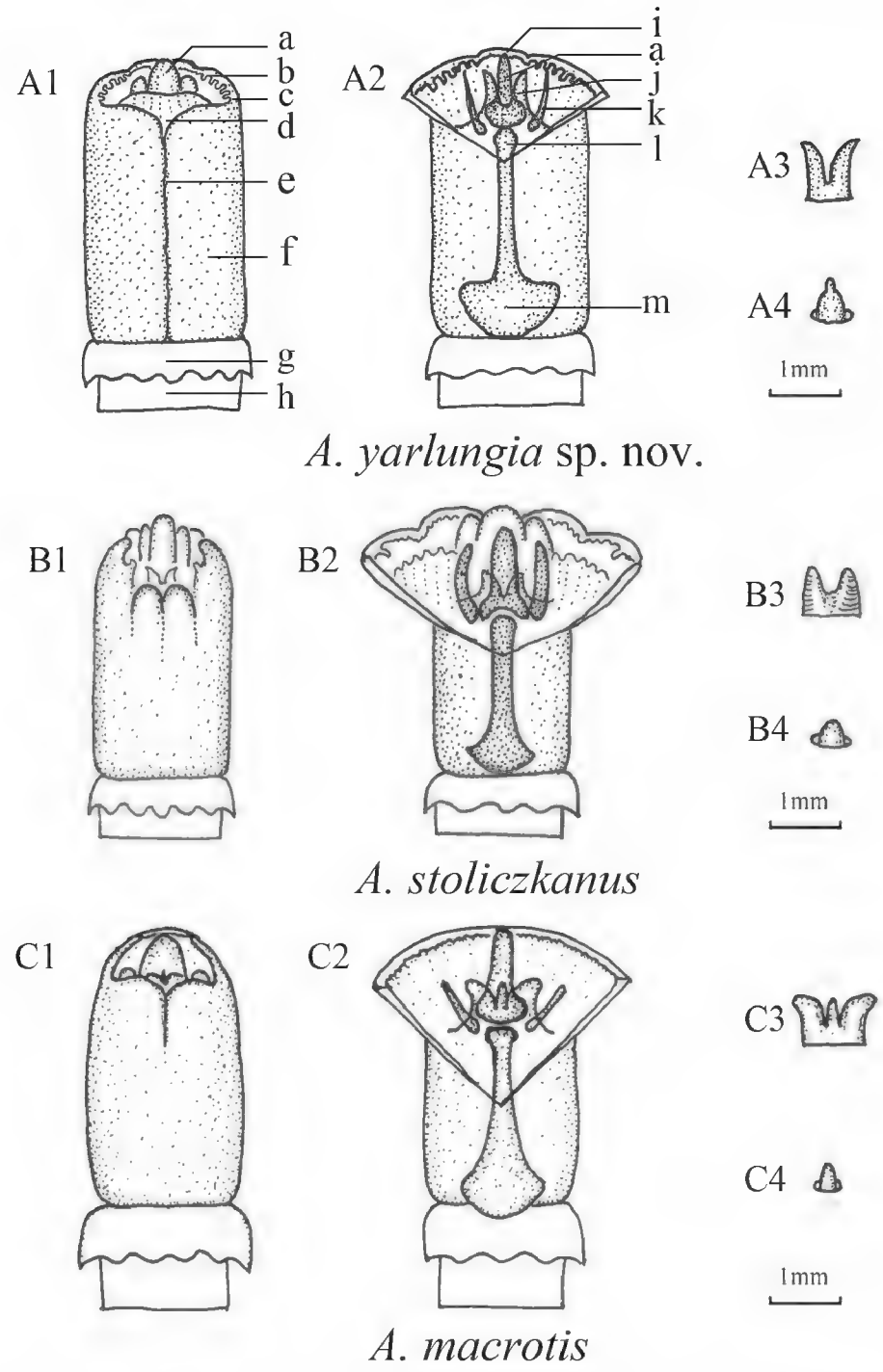

Figure 7. Comparison of the glans penis and baculum between *Alticola yarlungia* sp. nov. (**A**), *A. stoliczkanus* (**B**) and *A. macrotis* (**C**). Numerals indicate: 1, penis; 2, midventral cut view of glans; 3, urethral papilla; 4, dorsal papilla. Lowercase letters indicate: a, distal baculum; b, outer crater papillae; c, outer crater; d, urethral papilla; e, ventral groove; f, glans; g, prepuce; h, body of penis; i, tip of distal baculum; j, site of dorsal papilla; k, lateral baculum; l, proximal baculum; m, base of proximal baculum.

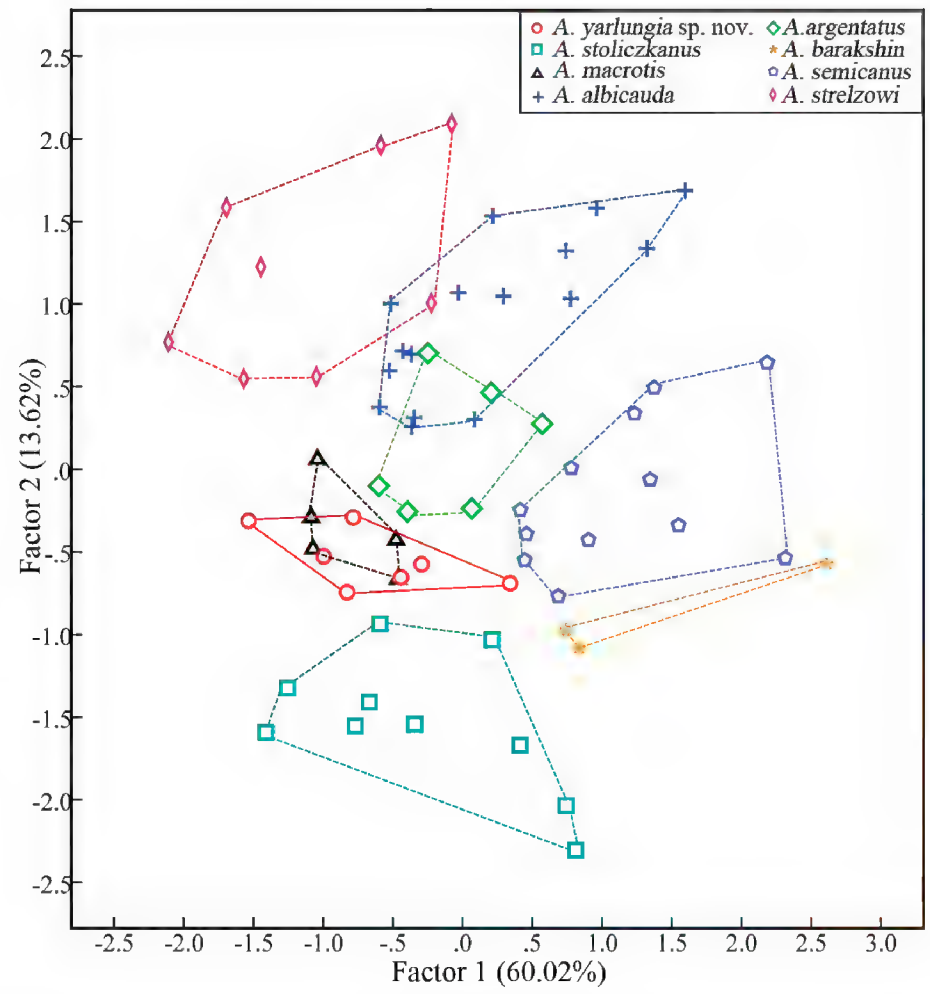

Figure 8. Scatterplot from factor analysis of morphometric data for eight congeners of *Alticola* distributed in China.

Alticola in China (Rossolimo et al. 1994), and it is more closely related to *A. yarlungia* sp. nov. (Figs 2–4, Table 1). Compared to *A. stoliczkanus*, *A. yarlungia* sp. nov. is larger in appearance (Table 2) and its tail is slender, longer, shorter haired, and darker in dorsal view (Fig. 5, Table 3). The M^3 of *A. stoliczkanus* is considered to be the shortest and simplest among *Alticola*, with two lingual angles and a very wide second labial side infold (Fig. 6B1; Rossolimo et al. 1994; Mead and Nadachowski 1999; Kryštufek et al. 2017). However, the M^3 of *A. yarlungia* sp. nov. exhibits an even simpler structure than that of *A. stoliczkanus*, primarily due to its significantly truncated posterior lobe. The posterior loop of *A. yarlungia* sp. nov. is shortened significantly relative to *A. stoliczkanus*, forming the third inner salient angle and the second inner reentrant (Fig. 6A1, B1). The M^3 pattern of *A. yarlungia* sp. nov. exhibits intraspecific variation; some specimens, such as GB828002, have slightly extended posterior loops, weak third inner angles and shallower second inner reentrant (Tang et al. 2018). M_3 has 4 closed loops in 50% specimens of *A. yarlungia* sp. nov., but most other species of *Alticola* do not have this characteristic, except for *A. stoliczkanus* (Luo et al. 2000; Tang et al. 2018). In terms of habitat, *A. yarlungia* sp. nov. occurs in shrubs near streams in elevations ranging from 3,228 m to 4,022 m. In contrast, *A. stoliczkanus* occurs in higher regions of mountain valleys above the timber line. It nests in heaps of stones and boulders of glacial moraines and also occupies areas entirely covered by grass at elevations ranging from 3,900 m to 5,450 m (Mead and Nadachowski 1999; Luo et al. 2000). Finally, the morphology of the glans penis and baculum provide further evidence to support the species status of *A. yarlungia* sp. nov. (Fig. 7), which differs from *A. stoliczkanus* and *A. macrotis* in its outer crater papillae, proximal, distal, and lateral bacula, urethral lappet, and dorsal papillae. These distinct morphological differences in the glans penis and baculum are consistent with reproductive isolation between *A. yarlungia* sp. nov. and each of its close relatives, *A. stoliczkanus* and *A. macrotis*.

Five species of *Alticola* are unknown in China (Wei et al. 2025). *Alticola yarlungia* sp. nov. differs from these congeners by TL/HBL ratio (*A. montosa* and *A. tuvinicus*), the first and second outer reentrant (*A. lemminus*), and the third and fourth inner angles of M^3 (*A. lemminus* and *A. olchonensis*), respectively (Table 3; Bolshakov et al. 2012). The terra typica of *A. roylei* Gray, 1842 is Kumaon, northern India. This species is recorded in the western Himalayas from Kulu Valley in Himachal Pradesh to northern Kumaon in Uttar Pradeshat, at elevations ranging from 2,600 m to 3,900 m (Musser and Carleton 2005). Occurring in Central Asia, *A. roylei* was once considered

the broadest-ranging species of *Alticola* especially when encompassing *A. argentatus* and many of its synonyms (Ellerman and Morrison-Scott 1951; Luo et al. 2000; Musser and Carleton 2005). Luo et al. (2000) believed four subspecies (*argentata*, *phasma*, *rosanovi* and *worthingtoni*) of *A. roylei* occurred in China. However, with the recognition of *A. argentatus*, the above-mentioned subspecies become synonyms of *A. argentatus* (Musser and Carleton 2005). So far, no reliable specimen of *A. roylei* has been collected in China. The diagnostic characteristics of *A. roylei* include a distinctly bicolored tail (with ratio 33–36% of HBL), heavy cheek teeth, well-developed third inner angle of M^3 (Hinton 1926; Kryštufek et al. 2017), all of which are different from *A. yarlungia* sp. nov. (Table 3).

In summary, the distinct species status of *Alticola yarlungia* sp. nov. is robustly supported by its position as a well-supported monophyletic clade, substantial K2P distances from congeners in *CYTB* (4.0–10.3%), and a suite of morphological traits (pelage, M^3, and baculum). This discovery underscores the underestimated diversity within *Alticola* and provides critical new insights into the genus's evolution. Given the contiguous transboundary habitats (Wang et al. 2024), *A. yarlungia* likely also inhabits the southern slopes of the eastern Himalayas. The vast and complex topography of this region warrants intensified surveys. Such efforts will likely uncover additional cryptic diversity and enhance the conservation value of this significant area.

Taxonomic account

Family Cricetidae Fischer, 1817
Genus *Alticola* Blanford, 1881

***Alticola yarlungia* Tang, Qiu, Peng & Liu, 2025, sp. nov.**
https://zoobank.org/EA04165B-4BAD-4D7F-A168-113B0C00B5C3

Holotype. Adult male, SAF 230697, collected by Rui Liao et al. on 27 August 2023 (field number XZ23458, summer pelage) using a snap trap. Collected in shrub habitat near Naijiaxiongqu (stream), Xibaxiaqu River, a right tributary of Yarlung Zangbo River. Specimen prepared as a skin with cleaned skull, baculum, and muscle tissue deposited at the Sichuan Academy of Forestry.

Measurements of holotype. Weight 29 g; HBL 104 mm; TL 24 mm; HFL 18 mm; EL 12 mm; SGL 24.77 mm; CBL 22.76 mm; ZB 13.35 mm; IOB 3.84 mm; NL 7.49 mm; HB 9.06 mm; M–M 4.81 mm; LMxT 14.44 mm; LUMR 5.12 mm; LLMR 5.29 mm; MGL 17.35 mm; ML 14.52 mm.

Type locality. San'anqulin Township, Longzi County, Lhoka City, Tibet Autonomous Region, China (28.59838°N, 92.92745°E; 4,022 m elev).

Paratypes. Six specimens (3 male, 3 female), skins with skulls, and male specimens with glans penis. Two topotype adult specimens collected on 27 August 2023: SAF 230699 (Field number XZ23460, male) and SAF 230700 (Field number XZ23461, female). Two adult specimens collected by Rui Liao et al. from Jindong Township, Lang County on 30 August 2023: SAF 230750 (Field number XZ23511, male) and SAF 230751 (Field number XZ23512, female), 28.94895°N, 93.38686°E, 3,228 m elev. One adult specimen collected by Rui Liao et al. from Jindong Township, Lang County on 30 August 2023: SAF 230743 (Field number XZ23504, male), 28.95136°N, 93.38714°E, 3,238 m elev. One adult specimen collected by Rui Liao and Ning Xing from Jindong Township, Lang County on 20 August 2008: SAF 081053 (Field number GB828002, female), 28.93505N, 93.39156E, 3,279 m elev. All six paratypes are deposited in the collections of the Sichuan Academy of Forestry.

Measurements of paratypes. Weight 20–40 g; HBL 92–107 mm; TL 23–28 mm; HFL 17–18 mm; EL 14–15 mm; SGL 23.43–26.2 mm; CBL 21.23–24.02 mm; ZB 11.71–14.2 mm; IOB 3.94–4.33 mm; NL 7.05–8.23 mm; HB 8.66–9.62 mm; M–M 5.03–5.26 mm; LMxT 13.83–15.54 mm; LUMR 5.32–5.85 mm; LLMR 5.43–5.77 mm; MGL 16–18.54 mm; ML 13.07–16.33 mm.

Geographic distribution. The species is known only from Longzi County, Lhoka City, and Lang County, Nyingchi City, Tibet, China.

Etymology. The specific epithet *yarlung* is a toponym derived from the Yarlung Zangbo River, the type locality of the new species (Longzi and Lang County), which drains this river basin, with the Latin suffix -ia denoting 'pertaining to' or 'from the region of'. The Yarlung Zangbo River is the largest river in Tibet, known for a very high diversity of elevations, habitats and species. We propose the English name "Yarlung Zangbo Mountain Vole" and the Chinese name "雅鲁藏布高山鼢 (Yǎlǔ Zàngbù Gāoshān Píng)" for this new species.

Diagnosis. A medium-sized species of *Alticola* characterized by the following combination of characters: HBL of adult 92–110 mm and TL comprises nearly one fourth of the HBL. Body back with obvious dark brown tinge, belly dirty white; tail slender and indistinctly bicolored, covered with short hairs that are brownish above and gray white below; shortened upper molar row, M^3 usually with two lingual reentrants, three lingual angles, two labial reentrants and three labial angles, with a shortened posterior lobe typically contacting to the third labial angle; M_3 with three loops, the middle loop being divided into two in approximately half of the specimens. *Alticola yarlungia* is geographically proximate to *A. stoliczkanus* and similar in general body coloration and tooth patterns. However, it differs in having a distinctly narrower second labial reentrant on M^3 and a more stable and pronounced second lingual reentrant. The new species is larger than *A. stoliczkanus* in several measurements, including HBL (102 ± 5.89 mm vs. 91.91 ± 3.91 mm), HFL (17.78 ± 0.67 mm vs. 16.91 ± 0.83 mm), and EL (14.44 ± 1.24 mm vs. 12.82 ± 0.4 mm). The tail is longer and more slender with shorter hairs and a shorter tufted tip (TL = 25.22 ± 1.79 mm, 24.8% of HBL; vs. 20.09 ± 1.87 mm, 21.9% of HBL in *A. stoliczkanus*).

Description. The general pelage color of holotype is brown, with the dorsal fur approximately 9 mm long. Proximal part of back fur black-gray, while distal parts brown. Ventral fur gray-white with a black-gray base, uniform color from throat to belly and anus, with a distinct color boundary between the dorsal and ventral fur. Pelage of paratypes same as that of the holotype. Mystacial vibrissae mostly white, but some are black, with approximately 26 mm on each side. Shortest vibrissa approximately 8 mm, and longest approximately 30 mm. Ears projected slightly above pelage. Pinnal rim entirely brown, with dense brown fur. Tail slender, covered with short hairs that extend for about 7 mm beyond tail-tip, color on top brown, lighter than dorsal fur, underside consistently gray whitish. Hairs on the tip of tail slightly longer. Foot covered with gray-white hairs; claws blackish-gray, with long, stiff hair, thumb vestigial and clawless. Palms with five, soles with six pads, black-brown. Females with two pectoral and two inguinal pairs of mammae (Fig. 5A).

Skull small and rounded in dorsal profile, nasal bones broad anteriorly and narrow posteriorly, tapering to appear elongated, and braincase approximately orbicular. Posterior and anterior frontal bones broad but narrow in interorbital region. Interparietal bone antero-posteriorly narrow, subtriangular. Post-orbital squamosal crests slightly weaker. Two ridges behind temporal joint above auditory bulla. Zygomatic arches sturdy. Auditory bullae medium-sized and globular. Posterior palate typical of Arvicolinae; structure of palate terminates in a square-edged, thin bony shelf, lacking upward-sloping bony bridge connecting median point with inner borders of both lateral pits. Palatine and pterygoid with numerous small foramina. Mandibles sturdy. Upper incisors straight with anterior faces light orange. M^1 with four closed triangles after anterior transverse space, forming three inner and three outer angles. M^2 with three closed triangles after anterior transverse space, forming two inner and three outer angles. M^3 comprises three main loops, forming three outer and three inner angles; the first transverse loop includes a shallow outer reentrant between two outer angles (former slightly exceeding latter) and salient inner angle; the second small loop with second inner angle, back to second outer deep reentrant; the third loop usually an anterior outer angle, middle inner angle and near circular terminal of substantially shortened posterior lobe, sometimes the posterior lobe moderately extending and the middle inner angle becoming weaker or absent. Lower incisors relatively long, and lip-side light orange. M_1 with four staggered triangles anterior to posterior transverse space; anterior space shorter and anomalistic, forming one inner and one outer angle, totally with four inner and four outer angles. M_2 bearing four closed loops and three inner and three outer angles. M_3 possesses three closed loops (sometimes the middle loop divided into two closed loops), forming three inner and three outer angles (Fig. 9).

Glans penis generally same size as other congeners (Fig. 7A). Four to five outer crater papillae on each side (Fig. 7A1, b), base of proximal baculum semicircular (Fig. 7A2, m), distal, lateral bacula slender (Fig. 7A2, a, k), and lateral bacula with a sharp tip (Fig. 7A2, k). Urethral lappet forked into two long branch forks with deep bifurcation (Fig. 7A3). Dorsal papillae with a distalis digitation (Fig. 7A4).

Habitat. This new species is expected to occur in primary or secondary forest with low cover, shrubs along the bank of valley. Elevation of the collected specimens ranges from 3,228 m to 4,022 m, lower than that of *A. stoliczkanus*. Nine specimens collected in sunny, riparian habitat near stream. Vegetation of the type locality consists of shrubs, averaging 2.0 m high, with 40% coverage along with grasses, about 0.3 m high, at 25% of coverage. Thickness of the humus layer is no more than 5 cm.

Figure 9. Craniodental morphology of the holotype of *Alticola yarlungia* sp. nov (voucher number: XZ23458). **A1.** Dorsal view; **A2.** Ventral view; **A3.** Lateral view; **A4, A5.** Mandible; **B1.** Right upper molar row (lingual side on right); **B2.** Right lower molar row (lingual side on left).

Acknowledgments

This work was supported by the National Natural Science Foundation of China (Grant Nos. 32370496 and 31970399), the 2024 Tianfu Qingcheng Plan Distinguished Scientist Program (Grant No. CQC-1843), and the Tibet Gongbu Nature Reserve Comprehensive Scientific Investigation Report Preparation Project. We acknowledge the Sichuan Center for Disease Control and Prevention (Chengdu) and the Xinjiang Center for Disease Control and Prevention (Urumqi) for providing specimens. We are grateful to Ning Xing for his assistance in field specimen collection.

References

Abramson NI, Lissovsky AA (2012) Subfamily Arvicolinae Gray, 1821. In: Pavlinov IY, Lissovsky AA (Eds) The mammals of Russia: a taxonomic and geographic reference. KMK Scientific Press, Moscow, 220–276.

Abramson N, Lebedev VS, Tesakov AS, Bannikova AA (2009) Supraspecies relationships in the subfamily Arvicolinae (Rodentia, Cricetidae): An unexpected result of nuclear gene analysis. Molecular Biology 43(5): 834–846. https://doi.org/10.1134/S0026893309050148

Allen GM (1940) The mammals of China and Mongolia. Natural History of Central Asia, Vol. XI. Part 2. American Museum of Natural History, New York, 621–1350.

Andreychev AV, Kuznetsov VA (2020) Checklist of rodents and insectivores of the Mordovia, Russia. ZooKeys 1004: 129–139. https://doi.org/10.3897/zookeys.1004.57359

Bodrov SY, Kostygov AY, Rudneva LV, Abramson NI (2016) Revision of the taxonomic position of the Olkhon Mountain vole (Rodentia, Cricetidae). The Biological Bulletin 43(2): 136–145. https://doi.org/10.1134/S1062359016020035

Bolshakov VN, Vasilyeva IA, Vasilyev AG (2012) Morphological Disparity among Rock Voles of the Genus *Alticola* from Mongolia, Kazakhstan and Russia (Rodentia, Cricetidae). Erforschung biologischer Ressourcen der Mongolei 12: 105–115.

Bouckaert R, Vaughan TG, Barido-Sottani J, Duchene S, Fourment M, Gavryushkina A, Heled J, Jones G, Kuhnert D, De Maio N, Matschiner M, Mendes FK, Muller NF, Ogilvie HA, du Plessis L, Popinga A, Rambaut A, Rasmussen D, Siveroni I, Drummond AJ (2019) BEAST 2.5: An advanced software platform for Bayesian evolutionary analysis. PLoS Computational Biology 15(4): e1006650. https://doi.org/10.1371/journal.pcbi.1006650

Castresana J (2000) Selection of conserved blocks from multiple alignments for their use in phylogenetic analysis. Molecular Biology and Evolution 17(4): 540–552. https://doi.org/10.1093/oxfordjournals.molbev.a026334

Cheng F, He K, Chen ZZ, Zhang B, Wan T, Li JT, Zhang BW, Jiang XL (2017) Phylogeny and systematic revision of the genus *Typhlomys* (Rodentia, Platacanthomyidae), with description of a new species. Journal of Mammalogy 98: 731–743. https://doi.org/10.1093/jmammal/gyx016

Dubey S, Salamin N, Ohdachi SD, Barriere P, Vogel P (2007) Molecular phylogenetics of shrews (Mammalia: Soricidae) reveal timing of transcontinental colonizations. Molecular Phylogenetics and Evolution 44(1): 126–137. https://doi.org/10.1016/j.ympev.2006.12.002

Ellerman JR, Morrison-Scott TCS (1951) Checklist of Palaearctic and Indian mammals, 1758 to 1946. British Museum (Natural History), London, 670–674.

Galewski T, Tilak MK, Sanchez S, Chevret P, Paradis E, Douzery EJ (2006) The evolutionary radiation of Arvicolinae rodents (voles and lemmings): Relative contribution of nuclear and mitochondrial DNA phylogenies. BMC Evolutionary Biology 6: 80. https://doi.org/10.1186/1471-2148-6-80

Gromov IM, Polyakov IY (1977) Voles (Microtinae), Fauna of the USSR, Mammals Vol. III, No. 8. Nauka Publisher, Leningrad, 504 pp. [In Russian]

Gu TT, Zhu WL (2025) Research advance in the genetics and adaptive evolution of small mammals on the Qinghai-Tibet Plateau. Chinese Bulletin of Life Sciences 37(6): 735–746. [In Chinese] https://doi.org/10.13376/j.cbls/2025073

He K, Li YJ, Brandley MC, Lin LK, Wang YX, Zhang YP, Jiang XL (2010) A multi-locus phylogeny of Nectogalini shrews and influences of the paleoclimate on speciation and evolution. Molecular Phylogenetics and Evolution 56(2): 734–746. https://doi.org/10.1016/j.ympev.2010.03.039

Hinton MAC (1926) Monograph of the voles and lemmings (Microtinae) living and extinct. British Museum (Natural History), London, 488 pp. https://doi.org/10.5962/bhl.title.8319

Holden ME, Cserkész T, Musser GG (2017) Family Sminthidae. In: Wilson DE, Lacher TE, Mittermeier RA (Eds) Handbook of the mammals of the world, Vol. 7: Rodents II. Lynx Ediciones, Barcelona, 299–308.

Hooper ET (1958) The male phallus in mice of the genus *Peromyscus*. Miscellaneous Publications (University of Michigan. Museum of Zoology) 623: 1–18. https://doi.org/10.3998/mpub.12946894

Hooper ET, Hart BS (1962) A synopsis of recent North American micortine rodents. Miscellaneous Publications (University of Michigan. Museum of Zoology) 120: 5–68. https://doi.org/10.3998/mpub.12946903

Kapli P, Lutteropp S, Zhang J, Kobert K, Pavlidis P, Stamatakis A, Flouri T (2017) Multi-rate Poisson tree processes for single-locus species delimitation under maximum likelihood and Markov chain Monte Carlo. Bioinformatics 33(11): 1630–1638. https://doi.org/10.1093/bioinformatics/btx025

Katoh K, Standley DM (2013) MAFFT multiple sequence alignment software version 7: Improvements in performance and usability. Molecular Biology and Evolution 30(4): 772–780. https://doi.org/10.1093/molbev/mst010

Kimura M (1980) A simple method for estimating evolutionary rates of base substitutions through comparative studies of nucleotide sequences. Journal of Molecular Evolution 16: 111–120. https://doi.org/10.1007/bf01731581

Kohli BA, Speer KA, Kilpatrick CW, Batsaikhan N, Damdinbazar D, Cook JA (2014) Multilocus systematics and non-punctuated evolution of Holarctic Myodini (Rodentia: Arvicolinae). Molecular Phylogenetics and Evolution 76: 18–29. https://doi.org/10.1016/j.ympev.2014.02.019

Kryštufek B, Shenbrot GI, Gregori J, Benda P, Hutterer R (2017) Taxonomic and geographic setting of Royle's mountain vole *Alticola roylei* revisited. Mammalia 81(5): 503–511. https://doi.org/10.1515/mammalia-2016-0102

Lanfear R, Calcott B, Ho SYW, Guindon S (2012) Partitionfinder: Combined selection of partitioning schemes and substitution models for phylogenetic analyses. Molecular Biology and Evolution 29(6): 1695–1701. https://doi.org/10.1093/molbev/mss020

Lebedev VS, Bannikova AA, Tesakov AS, Abramson NI (2007) Molecular phylogeny of the genus *Alticola* (Cricetidae, Rodentia) as inferred from the sequence of the cytochrome *b* gene. Zoologica Scripta 36: 547–563. https://doi.org/10.1111/j.1463-6409.2007.00300.x

Liu S, Liu Y, Guo P, Sun Z, Murphy RW, Fan Z, Fu J, Zhang Y (2012) Phylogeny of oriental voles (Rodentia: Muridae: Arvicolinae): molecular and morphological evidence. Zoological Science 29(9): 610–622. https://doi.org/10.2108/zsj.29.610

Liu SY, Chen SD, He K, Tang M, Liu Y, Jin W, Li S, Li Q, Zeng T, Sun ZY, Fu JR, Liao R, Meng Y, Wang X, Jiang XL, Murphy RW (2019) Molecular phylogeny and taxonomy of subgenus *Eothenomys* (Cricetidae: Arvicolinae: Eothenomys) with the description of four new species from Sichuan, China. Zoological Journal of the Linnean Society 186(2): 569–598. https://doi.org/10.1093/zoolinnean/zly071

Liu S, Liu Y, Meng G, Zhou C, Liu Y, Liao R (2020) A new record of a mammal in China and new provincial records in Xizang, Hubei and Sichuan. Acta Theriologica Sinica 40(3): 261–270. [In Chinese] https://www.mammal.cn/CN/10.16829/j.slxb.150354

Liu S, Tang M, Murphy RW, Liu Y, Wang X, Wan T, Liao R, Tang K, Qing J, Chen S, Li S (2022) A new species of *Tamiops* (Rodentia, Sciuridae) from Sichuan, China. Zootaxa 5116(3): 301–333. https://doi.org/10.11646/zootaxa.5116.3.1

Luo ZX, Chen W, Gao W (2000) Mammalia, Vol.6, Rodentia, Part III: Cricetidae. In: Luo ZX, Chen W, Gao W (Eds) Fauna Sinica. Science Press, Beijing, 333–388. [In Chinese]

Luo AR, Qiao HJ, Zhang YZ, Shi WF, Ho SYW, Xu WJ, Zhang AB, Zhu CD (2010) Performance of criteria for selecting evolutionary models in phylogenetics: A comprehensive study based on simulated datasets. BMC Evolutionary Biology 10: 242. https://doi.org/10.1186/1471-2148-10-242

Mead JI, Nadachowski A (1999) Alticola stoliczkanus. Mammalian Species 624: 1–4. https://doi.org/10.2307/3504506

Meng G, Li Y, Yang C, Liu S (2019) MitoZ: A toolkit for animal mitochondrial genome assembly, annotation and visualization. Nucleic Acids Research 47(11): e63. https://doi.org/10.1093/nar/gkz173

Musser GG, Carleton MD (1993) Muridae: Arvicolinae. In: Wilson DE, Reeder DM (Eds) Mammal species of the world: a taxonomic and geographic reference (2nd edn.). Smithsonian Institution Press, Washington, 501–536.

Musser GG, Carleton MD (2005) Superfamily Muroidea. In: Wilson DE, Reeder DM (Eds) Mammal species of the world: a taxonomic and geographic reference (3rd edn.). Johns Hopkins University Press, Baltimore, 894–1531.

Ognev SI (1962) Mammals of the USSR and adjacent countries Carnivora (in Russian; English translation by Birron A, Coles ZS for Israel Program for Scientific Translations).

Puillandre N, Brouillet S, Achaz G (2021) ASAP: Assemble species by automatic partitioning. Molecular Ecology Resources 21(2): 609–620. https://doi.org/10.1111/1755-0998.13281

Rambaut A, Drummond AJ, Xie D, Baele G, Suchard MA (2018) Posterior Summarization in Bayesian Phylogenetics Using Tracer 1.7. Systematic Biology 67(5): 901–904. https://doi.org/10.1093/sysbio/syy032

Repenning CA (1990) Arvicolid rodent biochronology of the Northern Hemisphere. In: Oldrich F, Wolf-Dieter H (Eds) International Symposium on the Evolution and Phylogenetic Biostratigraphy of Arvicolids (Rodentia, Mammalia). Pfeil-Verlag, Prague, 385–418.

Ronquist F, Huelsenbeck JP (2003) MrBayes 3: Bayesian phylogenetic inference under mixed models. Bioinformatics 19(12): 1572–1574. https://doi.org/10.1093/bioinformatics/btg180

Rossolimo O, Pavlinov IY, Hoffmann R (1994) Systematics and distribution of the rock voles of the subgenus *Alticola s. str.* in the People's Republic of China (Rodentia, Arvicolinae). Acta Theriologica Sinica 14(2): 86–99.

Serdyuk NV, Tesakov AS (2006) New form of rhizodont voles (Rodentia, Arvicolinae, Clethrionomyini) from Pleistocene of Central Altai (Russia). Russian Journal of Theriology 5(2): 79–83. https://doi.org/10.15298/rusjtheriol.05.2.05

Sikes RS, the Animal Care and Use Committee of the American Society of Mammalogists (2016) 2016 Guidelines of the American Society of Mammalogists for the use of wild mammals in research and education. Journal of Mammalogy 97(3): 663–688. https://doi.org/10.1093/jmammal/gyw078

Smith AT, Xie Y, Hoffmann RS, Lunde D, MacKinnon J, Wilson DE, Wozencraft WC, Gemma F (2010) A guide to the mammals of China. Princeton University Press, New Jersey, 576 pp. https://doi.org/10.1515/9781400834112

State Council Order of the People's Republic of China (1992) Regulations of the People's Republic of China on the Implementation of Terrestrial Wildlife Protection. The Ministry of Forestry of PR China. [In Chinese]

Tamura K, Stecher G, Kumar S (2021) MEGA11: Molecular evolutionary genetics analysis version 11. Molecular Biology and Evolution 38(7): 3022–3027. https://doi.org/10.1093/molbev/msab120

Tang MK, Jin W, Tang Y, Yan CC, Murphy RW, Sun ZY, Zhang XY, Zeng T, Liao R, Hou QF, Yue BS, Liu SY (2018) Reassessment of the taxonomic status of *Craseomys* and three controversial species of *Myodes* and *Alticola* (Rodentia: Arvicolinae). Zootaxa 4429(1): 1–52. https://doi.org/10.11646/zootaxa.4429.1.1

True FW (1894) Note on mammals of Baltistan and the vole of Kashmir, presented to the National Museum by Dr. W. L. Abbott. Proceedings of the United States National History 976: 1–16. https://doi.org/10.5479/si.00963801.976

Wang SY, Li YX, Li Q, Song WY, Wang HJ, He SW, Otieno Onditi K, Khanal L, Li XY, Chen ZZ, Jiang XL (2024) A new species of mountain vole (Rodentia, Cricetidae, Neodon) from south Xizang, China. Zoological Research, Diversity and Conservation 1(4): 282–289. https://doi.org/10.24272/j.issn.2097-3772.2024.011

Wei F, Yang Q, Wu Y, Jiang X, Liu S, Hu Y, Ge D, Li B, Yang G, Li M, Zhou J, Li S, Li S, Yu W, Chen B, Zhang Z, Zhou C, Wu S, Zhang L, Chen Z, Chen S, Deng H, Jiang T, Zhang L, Shi H, Lu X, Li Q, Liu Z, Cui Y, Li Y, He K (2025) Catalogue of mammals in China (2024). Acta Theriologica Sinica 45(1): 1–16. [In Chinese] https://www.mammal.cn/CN/10.16829/j.slxb.151039

Xia L, Yang QS, Ma Y, Feng ZJ, Zhou LZ (2006) A guide to the measurement of mammal skull III: Rodentia and Lagomorpha. Chinese Journal of Zoology 41(5): 68–71. [In Chinese]

Yang Z (2015) The BPP program for species tree estimation and species delimitation. Current Zoology 61(5): 854–865. https://doi.org/10.1093/czoolo/61.5.854

Yang QS, Xia L, Ma Y, Feng ZJ, Quan GQ (2005) A guide to the measurement of mammal skull I: Basic measurement. Chinese Journal of Zoology 40(3): 50–56. [In Chinese] https://doi.org/10.1360/982005-245

Zeng T, Jin W, Sun ZY, Liu Y, Murphy RW, Fu JR, Wang X, Hou QF, Tu FY, Liao R, Liu SY, Yue BS (2013) Taxonomic position of *Eothenomys wardi* (Arvicolinae: Cricetidae) based on morphological and molecular analyses with a detailed description of the species. Zootaxa 3682(1): 85–104. https://doi.org/10.11646/zootaxa.3682.1.3

Zhang TZ, Jiang F, Xu B, Li B, Liang CB, Gu HF (2022) Research advances in conservation and management of endangered mammals on the Qinghai-Tibet Plateau. Acta Theriologica Sinica 42(5): 490–507. [In Chinese] https://www.mammal.cn/CN/10.16829/j.slxb.150696

Supplementary material 1

Supplementary information 1

Authors: Ming Kun Tang, Hong Qiu, Bu Qing Peng, Rui Liao, Robert W. Murphy, Xu Ming Wang, Xuan Pan, Xin Wang, Shao Ying Liu

Data type: doc

Explanation note: **table S1.** Gene markers, primer sequences and best-fit models used for phylogenetic analysis in this study. **table S2.** Pairwise estimates of evolutionary divergence (*p*-distance) among *Alticola* taxa based on *CYTB*. **table S3.** Results of ANOVA and *post-hoc* comparisons (Tukey's or Tamhane's T2 test) among *Alticola yarlungia* sp. nov., *A. stoliczkanus*, and *A. macrotis* (**P* < 0.05, ***P* < 0.01).

Copyright notice: This dataset is made available under the Open Database License (http://opendatacommons.org/licenses/odbl/1.0/). The Open Database License (ODbL) is a license agreement intended to allow users to freely share, modify, and use this Dataset while maintaining this same freedom for others, provided that the original source and author(s) are credited.

Link: https://doi.org/10.3897/zse.101.170704.suppl1

Supplementary material 2

Supplementary information 2

Authors: Ming Kun Tang, Hong Qiu, Bu Qing Peng, Rui Liao, Robert W. Murphy, Xu Ming Wang, Xuan Pan, Xin Wang, Shao Ying Liu

Data type: xls

Explanation note: **appendix 1.** Sampling information including localities and GenBank accession numbers for specimens used in this study. **appendix 2.** Information on specimens used for morphological analysis (see methods for abbreviations).

Copyright notice: This dataset is made available under the Open Database License (http://opendatacommons.org/licenses/odbl/1.0/). The Open Database License (ODbL) is a license agreement intended to allow users to freely share, modify, and use this Dataset while maintaining this same freedom for others, provided that the original source and author(s) are credited.

Link: https://doi.org/10.3897/zse.101.170704.suppl2